

Baltic Sea Surface Temperature Analysis 2022: A Study of Marine Heatwaves and Overall High Seasonal Temperatures

Anja Lindenthal¹ and Claudia Hinrichs¹, Simon Jandt-Scheelke¹, Tim Kruschke¹, Priidik Lagemaa³, Eefke M. van der Lee², [Ilja Maljutenko³](#), Helen E. Morrison², Tabea R. Panteleit¹, Urmas Raudsepp³

¹Federal Maritime and Hydrographic Agency, Hamburg, 20539, Germany

²Federal Maritime and Hydrographic Agency, Rostock, 18057, Germany

³Department of Marine Systems, Tallinn University of Technology, Tallinn, 12618, Estonia

Correspondence to: Claudia Hinrichs (claudia.hinrichs@bsh.de); Helen E. Morrison (helen.morrison@bsh.de)

Abstract. In 2022, large parts of the Baltic Sea surface experienced the third-warmest to the warmest temperatures over the summer and autumn temperatures months since 1997. Warm temperature anomalies ~~are a precondition for~~ can lead to marine heatwaves (MHWs), which are discrete periods of anomalous high temperatures relative to the usual local conditions. Here, we describe the overall sea surface temperature (SST) conditions observed in the Baltic Sea in 2022 and provide a spatio-temporal description of surface MHW events based on remote sensing, model reanalyses and in-situ station data. ~~Most~~ The most MHWs, ~~four and~~ locally ~~even~~ up to seven MHW events, were detected in the western Baltic Sea and the Inner Danish Straits, where maximum MHW intensities reached values of up to 4.6 °C above the climatological mean. The ~~Northern~~ northern Baltic Proper and the Gulf of Bothnia were impacted ~~by~~ mainly by two MHWs at maximum intensities of 7.3 °C and 9.6 °C, respectively. Our results also reveal that MHWs in the upper layer occur at a different period than at the bottom layers and are likely driven by different mechanisms. ~~Results~~ Model data from ~~the case studies at~~ two exemplary stations, ‘Lighthouse Kiel (LT Kiel)’ and ‘Northern Baltic’, show a significant increase ~~of~~ in MHW occurrences, of +0.773 MHW events per decade at LT Kiel ~~from 1989 to 2022~~ and of +0.64 MHW events per decade ~~from 1993 to 2022~~ at Northern Baltic, between 1993 and 2022. Moreover, we discuss the expected future ~~increase of MHW occurrences is discussed~~ increased occurrence of MHWs based on a statistical analysis at both locations.

1 Introduction

Global warming has ~~manifested itself through the~~ led to an increase of ocean heat content (OHC) by about 350 ZJ in the upper 2000 meters from 1958 to 2019, with the year 2022 being the warmest on record as of this writing (Cheng et al., 2022; WMO, 2023). Simultaneously, marine heatwaves (MHWs), ~~the~~ extreme events of high water temperature (Hobday et al., 2016), have increased in ~~their~~ frequency, duration, spatial extent and intensity during the past four decades (Sun et al., 2023). In 2022, MHWs were recorded on 58 % of the ocean surface (WMO, 2023).

29 The global mean air temperature in 2022 was 1.15 [1.02–1.28] °C above the 1850–1900 average, resulting in the year 2022 to
30 be the fifth or sixth warmest year in the 173-year instrumental record (WMO, 2023). We could hence expect the marginal seas
31 like the Baltic Sea to experience high sea surface temperatures (SST) as well. This hypothesis is supported by the study which
32 showed that the extremely warm weather conditions in winter 2019/20 resulted in an unusually high heat content anomaly in
33 the upper 50 m layer of the Baltic Sea (Raudsepp et al., 2022). Thus, a large scale weather pattern could have a detectable
34 response to the physical conditions of the Baltic Sea.

35 ~~Belkin (2009) showed that the Baltic Sea is one of the seas which have warmed marine ecosystems with the fastest in the last~~
36 ~~decades with a recorded~~ warming of surface temperatures of 1.35 K °C between 1982 and 2006, i.e., 0.54 °C per decade. ~~In our~~
37 ~~BSH (Belkin, 2009). SST~~ data (operationally produced by the German Federal Maritime and Hydrographic Agency (in the
38 following BSH, product ref. no. 1 in Table 1) ~~we see~~ show a warming trend of 0.58 °C per decade for the period 1990–2022
39 (based on annual means derived from satellite data, not shown). Local air-sea heat exchange is the main physical factor that
40 determines the surface layer water temperature and heat content in the Baltic Sea (Raudsepp et al., 2022). A permanent
41 halocline at the depth of 60–80 m (Väli et al., 2013) limits heat exchange between surface and lower layers. Further on, limited
42 water exchange of the Baltic Sea with the open ocean through the Skagerrak potentially reduces heat transport between the sea
43 and the ocean.

44 ~~MHWs are usually detected using remotely sensed SST.~~ High SST could SSTs can affect phytoplankton production, while
45 unprecedented high temperatures in the subsurface layers of the sea could have even more devastating effects on the marine
46 ecosystem (Kauppi et al., 2023). ~~Subsurface layer MHWs can be detected using temperature moorings, though unfortunately~~
47 ~~these moorings provide only point measurements. Numerical models enhance the possibility for studying dynamics of MHWs~~
48 ~~including their extension to the subsurface layers of the ocean. In this study we utilize remote sensing, model reanalyses and~~
49 ~~in situ station data for the spatio-temporal description of the MHWs in the Baltic Sea in 2022. So far, there are generally only~~
50 ~~a few studies about MHWs in the Baltic Sea (Goebeler et al., 2023). Conditions that facilitate the fast warming of the Baltic~~
51 ~~Sea are the limited exchange between surface and deeper layers due to a permanent halocline at a depth of 60–80 m (Väli et~~
52 ~~al., 2013) and the limited water exchange between the Baltic Sea and the open ocean through the narrow Skagerrak. That is~~
53 ~~why local air-sea heat exchange is the main physical factor for the surface layer water temperature and heat content in the~~
54 ~~Baltic Sea (Raudsepp et al., 2022), 2022; She et al., 2020).~~ In addition to the detailed description of MHWs in 2022 we extended
55 our study by providing climatology of the MHWs based on mooring station data.

56 ~~Maps~~ Global mean air temperature in 2022 was among the six warmest in the 173-year instrumental record (WMO, 2023). For
57 Europe especially, the Copernicus Climate Change Service/ECMWF (2022a) states that the air temperatures in August 2022
58 were higher than the 1991–2020 average across most of the continent, especially in a band in Eastern Europe stretching from
59 the Barents and Kara seas to the Caucasus. In November 2022, air temperatures were higher than the 1991–2020 average,
60 especially over the west, south-east and far north of Europe, and were unusually mild over the northern European seas
61 (Copernicus Climate Change Service/ECMWF, 2022b). These large-scale weather patterns likely lead to high sea surface

temperatures (SST) in marginal seas like the Baltic Sea and are a likely driver of MHWs. This hypothesis is further supported by a study by Holbrook et al. (2019), which found that MHWs at middle and high latitude regions were driven by large-scale atmospheric pressure anomalies which cause anomalous ocean warming. Stalled atmospheric high-pressure systems coincide with clear skies, warm air, and reduced wind speeds. These conditions then lead to quick warming of the upper ocean and increased thermal stratification due to reduced vertical mixing.

So far, there generally have been only a few studies on MHWs in the Baltic Sea (Goebeler et al., 2022; She et al., 2020). In this study, we show that remote sensing data revealed several SST anomalies over the entire Baltic Sea in 2022. We thus use model reanalysis and in-situ station data to provide a spatio-temporal description of the corresponding MHWs. Both datasets contain data collected over a long enough period to also provide its own respective climatology, thereby enabling a consistent representation of MHWs. While the in-situ data provides accurate point-wise measurements of the temperature at selected locations, the model reanalysis data allows for a widespread analysis of MHWs over the entire Baltic Sea, including their extension into subsurface layers. Furthermore, we extend our study by providing a climatology of MHWs at two specific mooring locations, namely at the Lighthouse Kiel (LT Kiel) and Northern Baltic stations. The overall aim of this study is to highlight the areas of the Baltic Sea that were (most) affected by MHWs and determine whether surface MHWs can propagate into deeper layers and thus potentially threaten the subsurface ecosystem. Furthermore, analyzing the climatology of MHWs can provide insight into whether the global increase in MHWs can also be expected to occur on a local scale for the Baltic Sea.

2 Data and Methods

2.1 Satellite data

The satellite data service at the BSH compiles daily maps of SST data (product ref. no. 1 in Table 1). These have contributed for example, used to studies by the BACC Author Team (2008) and Gröger et al. (2022), are compiled daily by the satellite data service at BSH (product ref. (2022). The SST no. 1 in Table 1). These data are recorded as radiances by the third-generation of the Advanced Very High Resolution Radiometer (AVHRR/3) in channels 4 and 5 centered at wavelengths 10.8 μm and 12.0 μm in the two thermal infrared respectively (EUMETSAT, 2015). The AVHRR/3 instruments used are flown channels aboard the polar orbiting NOAA-19 and MetOp B satellites, providing a spatial resolution of 1.1-km directly below the instrument (in nadir), swath widths of 1,447-km and orbital periods of 100 minutes (EUMETSAT, 2015; Minnett et al., 2019). This results in generally 8 or 9 daytime passes over the Baltic and North Sea area per day. The raw data (level 0) are received directly from EUMETSAT 90 minutes after flyover and processed using automated, standardized correction procedures (atmospheric correction, cloud masking, georeferencing etc.). Additionally, each flyover is corrected manually in order to preserve as much data as possible whilst eliminating any faulty or cloudy pixels. All available single images from a calendar day are combined and averaged, on a single pixel basis, into one daily-mean image. These daily images

92 are then used to produce a weekly analysis on an operational basis. ~~This weekly analysis is produced on an equidistant grid of~~
93 ~~58 by 74 cells in 20 km resolution, making use of an oblique Lambert projection with an origin at 56° N, 4° W (center of the~~
94 ~~BSH North Sea SST analysis). All daily satellite pixels falling into a 20x20 km grid box are considered equally when~~
95 ~~calculating a weekly average for this particular 20x20 km grid box. Eventually, the result for the weekly average is smoothed~~
96 ~~using a binomial filter (50 % weight for the grid box itself, 50 % for its respective neighbors).~~ While the BSH has been carrying
97 out the processing of the satellite data itself on the 1.1 km grid ~~has been carried out at BSH~~ since 1990, ~~the~~ operational SST
98 analysis for the Baltic Sea did not start until the autumn of 1996. The analysis of the BSH SST dataset presented in this chapter
99 is therefore ~~constrained~~limited to the period from 1997–2022.

100 2.2 Station data

101 In-situ temperature time series from mooring stations ~~which are~~ located in the Baltic Sea are ~~obtained from product ref. used~~
102 ~~for 1) model validation and 2) cross validation of the MHW computation from model data. Except no. 2 in Table 1, except~~ for
103 SST data from Northern Baltic (K. Hedi, FMI, pers. communication), ~~the station data are obtained from product ref. no. 2 in~~
104 Table 1. Each available dataset has already been quality controlled by the regional production units (In Situ TAC partners,
105 2022). The temporal resolution varies from hourly ~~data~~ at the German stations ~~and to~~ half-hourly at the stations in the northern
106 Baltic Proper and Gulf of Finland. Due to failures, maintenance and other circumstances, no mooring station entirely covers
107 the period from 1st Jan 1993 until now ~~entirely~~.

108 ~~From~~Of all available mooring stations, ~~those are~~we selected those which contain data from 2022 and from at least ten additional
109 years from 1993 until 2021 ~~in~~ at least one depth. Out of the ~~then~~ remaining seven mooring stations that contained surface
110 temperature data, two mooring stations were chosen for the ~~additional model~~cross validation ~~and the analysis~~ of MHWs:
111 Lighthouse Kiel (LT Kiel) and Northern Baltic. ~~(Fig. 1). Of the observation data, LT Kiel has the largest~~greatest time coverage
112 ~~of observation data (rather continuously from (1989 until the present). It, missing data: 9.1 % of days). This mooring station~~
113 lies in the far western part of the southern Baltic, and the water depth ~~at this mooring station there~~ is about 12 m. ~~On the other~~
114 ~~hand, The station~~ Northern Baltic is located in the northern Baltic Proper ~~and provides measurements down to water depths of~~
115 ~~103.8 m.~~ The SST observations there cover the period from 1997 until now, ~~rendering it an ideal candidate for evaluating the~~
116 ~~effects of MHWs into~~ (missing data: 8.0 % of days). ~~No mooring station provides a time series in deeper layers long or~~
117 ~~consistent enough to analyze subsurface MHWs, thus reducing the scope of measurement-based analysis of MHWs to the~~
118 surface layers.

119 2.3 Baltic Sea Physics Reanalysis Data

120 The Baltic Sea physics reanalysis product (product ref. no. 3 in Table 1) is a model dataset ~~produced by using~~based on the
121 ocean model NEMO v4.0, ~~a state-of-the-art oceanographic modeling framework~~ (Gurvan et al., 2019). The model system

122 assimilates satellite observations of SST (EU Copernicus Marine Service Product, 2022b) and in-situ temperature and salinity
123 profile observations from the ICES database (ICES Bottle and low-resolution CTD dataset, 2022). The product provides
124 gridded information on SST and subsurface temperature conditions. The spatial coverage is 1 ~~nm and~~ nautical mile, i.e.,
125 approximately 1.8 km. The grid covers the entire Baltic Sea, including the transition zone to the North Sea, with a vertical
126 resolution of 56 non-equidistant depth levels. This multi-year product (MYP) covers the reference period from 1993 up to
127 2022. The model setup is described in the Product User Manual (PUM, Ringgaard et al., 2023).

128 **2.4 Model validation**

129 ~~Although the Baltic Sea physics reanalysis product (product ref. no. 3 in Table 1) has already been extensively validated in the~~
130 ~~corresponding Quality Information Document (QuID; Panteleit et al., 2023), the model data is additionally validated for this~~
131 ~~chapter at different mooring stations, in particular LT Kiel and Northern Baltic, using the available station data (product ref.~~
132 ~~no. 2 in Table 1) and the full reference period from 1993 to 2022. Hence, in this case, only mooring stations were validated~~
133 ~~which are mostly located in the southern Baltic, whereas the validation in the QuID also considered ICES data which covered~~
134 ~~the entire Baltic Sea. Our evaluation confirms the results from the QuID, for example, that the MYP underestimates the~~
135 ~~temperature at the surface which, on average, results in a negative bias. Nevertheless, as can be clearly seen in Fig. 1, the~~
136 ~~temperature curves at Northern Baltic and LT Kiel, respectively, show the same progression. The generally lower temperature~~
137 ~~in the MYP results in a slightly lower temperature climatology and threshold (here, the 90th percentile), respectively, on which~~
138 ~~the MHW detection is based. In general though, the MHWs and their respective intensities and lengths are detected equally in~~
139 ~~both the station and model data.~~

140 ~~While the bias at the surface is between $-0.46\text{ }^{\circ}\text{C}$ and $-0.2\text{ }^{\circ}\text{C}$, the bias at deeper levels shifts towards more positive values. At~~
141 ~~the deepest levels where observational data is available, the bias in our validation ranges from $-0.22\text{ }^{\circ}\text{C}$ to $0.43\text{ }^{\circ}\text{C}$ which also~~
142 ~~corresponds to the results in the QuID ($-0.36\text{ }^{\circ}\text{C}$ to $0.26\text{ }^{\circ}\text{C}$). This means that the model bias varies at depth and with that~~
143 ~~maybe also the accuracy. To ensure the quality of the used station data from Northern Baltic, the validation of the lower level~~
144 ~~at the station BMPH2 from the QuID can be used as an approximation. BMPH2 is located only 43 km from Northern Baltic~~
145 ~~and reaches a depth of 150 m (in contrast to Northern Baltic with 105 m). It is a monitoring station which is operated by vessels~~
146 ~~and CTD casts are used to obtain measurements. These casts provide measurements at multiple depths, but are unevenly~~
147 ~~distributed over time (Panteleit et al., 2023). Unfortunately, there is no observation data available after 2019. With a bias of~~
148 ~~$0.15\text{ }^{\circ}\text{C}$ and a centered pattern root mean square difference (cRMSD) of $0.17\text{ }^{\circ}\text{C}$ the model data fits quite well to the station~~
149 ~~data (Fig. 1).~~

2.5 Heat wave detection

Marine heatwaves (MHWs) refer to a discrete period of unusually high seawater temperatures. While ~~there are~~ several definitions ~~to describe MHWs~~ quantitatively describe MHWs, the most commonly used method defines them as periods when temperatures exceed the 90th percentile of the local climatology for five days or more (Hobday et al. 2016). ~~Here, we apply the python package for MHW detection and statistics by~~ We use open-source tools to detect MHWs (Oliver et al., 2016) to the observational data and the Matlab package by Zhao and Marin ~~(, 2019) for the MHW statistics based on the in station and model data. These packages have been shown to produce identical results (Zhao and Marin, 2019).~~ The classification of identified MHWs follows can be classified following Hobday et al. (2018), wherein which the resulting MHW category is based on the maximum intensity in multiples of threshold exceedances, i.e., the local difference between the 90th percentile threshold and the climatology. If the threshold is exceeded by less than 2 times ~~this local difference~~, the MHW is classified as moderate (Category I), at 2 to 3 times it is classified as strong (Category II), at 3 to 4 times it is classified as severe (Category III), and at 4 ~~times~~ or more times it is classified as extreme (Category IV).

~~For~~ Here, the assessment occurrence of MHWs in the Baltic ~~domain during Sea in 2022 (Sect. 3.2), the climatological data of 1993 to 2022 as well as the data of 2022 are collected from~~ is analyzed based on the Baltic Sea MYP (product ref. no 3 in Table 1). The following statistical metrics of MHWs are computed at ~~each available~~ every third surface grid point of the ~~reanalysis MYP, resulting in a resolution of approximately 5.4 km~~: cumulative intensity, mean intensity, duration of the longest heatwave, number of heatwaves (frequency), maximum intensity and total days of MHW conditions.

~~In~~ Then, in order to evaluate the development of those MHW metrics over time, block averages (using a block length of one year) for each MHW metric are computed for ~~the time series data at the two mooring stations, for~~ both the observations (product ref. no 2 in Table 1) and the model data. ~~We then also compute the linear trend (95% (product ref. no 3 in Table 1) at two stations: Lighthouse Kiel and Northern Baltic. The yearly MHW metrics from observations and the model are correlated for evaluation, and linear trends (95% significance) are calculated~~ for each of those ~~annual MHW~~ metrics. Finally, the correlation of the annual MHW metrics to the annual mean temperature based on model data was assessed using a linear least-squares regression and a two-sided t-test for significance.

All MHW assessments in the following sections use the period from 1993 to 2021 for the climatology, except for Sect. 3.2.1, in which the comparison of the multi-year evolution of MHWs at Northern Baltic uses the overlapping period from 1997 to 2021 due to the lack of observations at this station before 1997.

2.5 Model validation

The MYP data has already been extensively validated in the corresponding Quality Information Document (QuID; Panteleit et al., 2023). In this document, the MYP data are validated within the time period from 1st January 1993 to 31st December 2018. The validation shows a negative bias at the surface with a shift towards more positive values at deeper levels. A variation

181 of statistical values with depth is also clearly visible in the estimated accuracy number (EAN), which represents the root-mean
182 square difference (RMSD) of a specific depth layer. The RMSD varies between 0.29 °C at 200–400 m over 0.63 °C at the
183 surface to 1.3 °C at 5–30 m depth.

184 We additionally evaluated the model data in more detail using a clustering approach, which offers insights into the overall
185 accuracy of the model by grouping the errors. This clustering procedure employs the K-means algorithm (Raudsepp and
186 Maljutenko, 2022). In this evaluation, all available data within the model's domain and simulation period are considered. A
187 two-dimensional error space (dS , dT) is established using simultaneously measured temperature and salinity values as the
188 foundation for clustering. Here, $dS=(S_{\text{mod}}-S_{\text{obs}})$ and $dT=(T_{\text{mod}}-T_{\text{obs}})$ represent the differences between the model (S_{mod} and T_{mod})
189 and observed (S_{obs} and T_{obs}) salinity and temperature, respectively. The dataset employed in this validation study was sourced
190 from the EMODNET dataset compiled by SMHI (product ref. no. 4 in Table 1). It consists of a total of 3,094,089 observations
191 aligning with the simulation period of the Baltic Sea physics reanalysis (product ref. no. 3 in Table 1) and covering the years
192 1993 to 2022. A comprehensive explanation of the k-means-method and detailed results describing the model's accuracy can
193 be found in Appendix A1. The results can be summarized as in that approximately 82 % of all validation points exhibit
194 relatively low temperature bias, STD, and RMSD (Table A1). The surface layer validation shows that less than 10 % of
195 comparison points have significant temperature errors (Figure A1c). Due to the low proportion of these validation points we
196 do not expect a significant impact on the determination of the surface MHWs and their statistics. Below the surface layer, i.e.,
197 at depths ranging from 0.5–40 m, up to 25 % of the points correspond to clusters with temperature errors greater than +/-
198 2.0 °C; in deeper layers, this percentage gets smaller again (Figure A1c). Consequently, we anticipate that the model reanalysis
199 data provide sufficiently accurate information for calculating subsurface MHWs and their statistics for the Baltic Sea as well.
200 The model is also validated in terms of how accurately it reproduces the MHWs of 2022 and how well it represents their
201 characteristics during the overlapping time periods of data availability at the two locations (1993–2022 for LT Kiel, and 1997–
202 2022 for Northern Baltic). For this, the model data was compared to the available station data (product ref. no 2 in Table 1 for
203 LT Kiel and K. Hedi, FMI, pers. communication for Northern Baltic) at these locations. Table 2 shows the Pearson correlation
204 coefficients for the MHW metrics in Fig 4 between observational and model data for the two stations, which show overall
205 good agreement between the model and the observation data with respect to MHW detection.

206 We also compared the annual temperature curves resulting from both the model and the station data at each location (Fig. A2).
207 Overall, the curves show the same progression. The temperature from the MYP is generally slightly lower, and consequently
208 this results in a slightly lower temperature climatology and threshold (here, the 90th percentile) on which MHW detection is
209 based. In general, though, the MHWs and their respective intensities and lengths are detected equally in both the station and
210 model data.

211 3 Results

212 3.1 Sea surface temperature anomalies in satellite data

213 ~~During~~In the summer ~~months of 2022~~, large parts of the Baltic Sea featured strong warm anomalies based on the BSH SST
214 analysis (product ref. no. with 1 in Table 1, Fig. 2). The highest values ~~of were~~ up to 3 °C above the long-term mean (1997–
215 2021) in the Bothnian Sea in June and in the Bothnian Bay in July, ~~respectively (Fig. 2)~~. In August however, these areas
216 ~~exhibit rather were~~ neutral ~~to or exhibited~~ cold anomalies, while the Baltic Proper as well as the Gulf of Finland and the Gulf
217 of Riga showed the warmest anomalies of +1.5 °C to 2.5 °C. ~~In~~At the beginning of autumn, the Baltic Sea is marked by a
218 substantial east-to-west gradient ~~regarding of~~ SST anomalies. ~~This is~~ due to a series of upwelling events along ~~the its~~ eastern
219 ~~coastlines of the Baltic Sea shores~~. In November, ~~again~~ the whole Baltic Sea features strong warm anomalies, again with peak
220 values above +2 °C around Southern Sweden.

221 To provide some climatological context ~~of for~~ the observed SST anomalies in a straightforward way, we also present maps
222 ~~of ranking~~ the SST ~~anomaly ranks~~ anomalies for the summer and autumn months ~~in of~~ 2022 ~~when compared to their~~
223 ~~respective~~ against the same months in previous years (right two columns of Fig. 2). ~~It is obvious that the warm anomalies found~~
224 2). These anomaly rankings provide information on how extreme an anomaly of a given magnitude is. For every grid point
225 and for each calendar month, the monthly anomalies are ranked by magnitude. The warm anomalies over large parts of the
226 Baltic Sea during the summer and autumn of 2022 belong to are among the warmest eight on record for the respective months.
227 ~~Except for~~In September ~~when the, coastal~~ upwelling ~~along the eastern coastlines~~ led to cold anomalies ~~contrasting the warm~~
228 ~~anomalies in the western half of the Baltic Sea, it is found for basically all along the eastern shores, but the~~ other five months
229 ~~of the summer and fall of 2022~~ (June ~~through, July and~~ August, as well as October and November) ~~that show~~ large areas of the
230 Baltic Sea ~~featured with~~ warm anomalies belonging to that are among the highest four most pronounced on record. ~~For~~In August
231 and November, we ~~even find see~~ several larger ~~of~~ areas along the coastlines s of the Baltic countries as well as off the Polish coast
232 and around Gotland that ~~featured surface temperatures being the highest ever~~ according to the BSH SST analysis (product ref.
233 dataset featured highest-ever surface temperatures. no. 1 in Table 1).

234 3.2 Marine heatwaves

235 ~~Temperature MHWs describe exceptionally warm temperature~~ anomalies ~~are a precondition for MHWs. The.~~ As the monthly
236 overview in Fig. 2 already provides an indication of possible MHW conditions. ~~To begin with, these are assessed by using the~~
237 ~~statistical-~~ in 2022, the MHW metrics defined by Hobday et al. (2016) at each grid point based on the SST data extracted
238 ~~from are assessed using~~ the Baltic Sea MYP (product ref. no. 3 in Table 1). Each region of the Baltic Sea experienced different
239 MHW characteristics during 2022 (Fig. 3), Table 3).

240 The most MHWs during 2022 ~~were detected~~ occurred in the Inner Danish Straits and the Western Baltic (Fig. 3d). ~~Mainly 4);~~
241 mainly, four to five MHWs were detected. ~~At, with~~ some assessed grid points, locations experiencing up to seven MHWs

242 ~~are detected, which leads to and~~ a maximum of ~~9694~~ total days of MHW conditions ~~in that area~~ (Fig. 3f). The mean and
243 maximum intensity~~s~~ of all ~~heatwaves~~MHWs in ~~these areas~~the Western Baltic reached up to 3.8 °C and 4.6 °C, respectively
244 (Fig. 3b and 3e). The highest ~~values in~~mean and maximum intensity ~~of MHWs~~values were reached in the ~~N~~northern Baltic
245 Proper (up to 5.3 °C, resp. 7.3 °C) as well as the Gulf of Bothnia (up to 6.5 °C, resp. 9.6 °C)~~and in the Bothnian Sea and~~
246 ~~Bothnian Bay (Fig. 3b and 3e), though these regions were affected mainly by only two MHWs.~~ The maximum ~~intensities were~~
247 ~~even~~intensity in the Bothnian Bay even reached 9.6 °C, the highest within the entire studied period from 1993 to 2022. ~~Those~~
248 ~~regions were impacted by mainly two MHWs, but at some individual grid points up to six MHWs are identified with a~~
249 ~~maximum value of up to 63 days with MHW qualification. While the duration of the~~The longest MHW is similar in both
250 ~~regions (Fig. found in the Baltic Proper (32 days), followed by the Bothnian Sea (31 days) and the Inner Danish Straits (29~~
251 ~~days) (Fig. 3c).~~ The highest values of cumulative intensity (of a single MHW) are found in the Gulf of Bothnia in the Kvarken
252 (), with up to 119.3 days °C), while the values in the Western Baltic and Inner Danish Straits are lower (up to 64 days °C) (Fig.
253 , are found in the Kvarken, a strait between the Bothnian Sea and ~~3a~~).

254 Compared with Fig. 2, the ~~Bothnian Bay (Fig. 3a)~~MHW with the highest cumulative intensity in the Gulf of Bothnia derives
255 from the temperature anomaly in November. The numerous MHWs in the Western Baltic and the large number of days with
256 MHW conditions connected with them occurred in both the summer and autumn months.

257 3.2.1 Multi-year evaluation of MHW metrics

258 Next, we assess the frequency and other characteristics of ~~the~~ MHWs that occurred in 2022 in a climatological context based
259 on both observations and model data for the two stations, LT Kiel (~~for~~based on the overlapping climatology period 1993–
260 2022~~1~~, Fig. 4a–h) and Northern Baltic (~~for~~based on the overlapping climatology period 1997–2022~~1~~, Fig. 4 i–p). Overall, the
261 results for the yearly MHW metric calculation are well correlated between the observations and the model data (Table 2).
262 In 2022, ~~in a~~ total of five MHWs (four in the MYP) occurred throughout the year at LT Kiel, ~~spread out through the year~~
263 (Fig. ~~1a~~A2a). Though none of ~~the 2022 MHWs~~them was extraordinarily long or intense at LT Kiel, the station datatime series
264 of yearly MHW metrics shows that, based on observational data, the number of MHW occurrences in 2022 was the second
265 highest after 2020there since 1989 (Fig. 4a). The time series of MHW frequency~~s~~ per year suggests that the occurrence of
266 MHW events has increased over the last three decades (Fig. 4a). ~~This~~ trend of computed from model data is +0.773 MHWs
267 per decade ~~becomes statistically significant when all for~~ the available station data from 1989period 1993–2022 is taken into
268 account. The number of MHW events per year is positively correlated (R=0.76) with the increasing annual mean SST at that
269 mooring station (Fig. 4b). The maximum (Fig. 4c) and cumulative intensities (Fig. 4e) of observed MHWs do not show a clear
270 trend and are not correlated to risingthe warming annual mean temperatures (Fig. 4d and Fig. 4f). There is no significant trend
271 in total MHW days (Fig. 4g) at LT Kiel, but a positive correlation (R=0.71) with rising average temperatures (Fig. 4h).

272 For Northern Baltic, neither the station data nor the model data exhibits a statistically significant trend in MHW events for the
273 overlapping period (Fig. 4i). But when all of the available model data from 1993–2022 is taken into account, the trend in MHW
274 occurrences becomes significant at the 95 % level, with +0.64 MHWs per decade. Again, the number of events is positively
275 correlated with annual mean temperature ($R=0.58$, Fig. 4j). The highest maximum MHW intensities were recorded in recent
276 years (2016, 2018, 2021, 2022), with 2022 showing the highest intensity of ~~any~~ MHW ~~with, at~~ 7.3 °C (model data) to 7.4 °C
277 (station data) above the climatologically expected temperature (Fig. 4k,l, see also Fig. ~~4bA2b~~). The cumulative MHW
278 intensities show no clear trend or correlation with annual mean temperatures at this station (Fig. 4m,n). In terms of total MHW
279 days, 2018 ~~was exceptional~~ shows the highest numbers (Fig. 4o), but otherwise no trend is detectable for this metric, though
280 there is positive correlation with annual mean temperatures ($R=0.56$, Fig. 4p).

281 3.2.2 Analysis of vertical MHW distribution at Northern Baltic

282 At Northern Baltic, which is ~~more than 104~~ about 103 m deep and located in the Western Baltic Proper, the surface temperature
283 has been measured continuously ~~measured~~ over several decades. Unfortunately, no quality-controlled temperature
284 measurements exist ~~in for the~~ lower layers. ~~In Sect. 2.4 we showed that the~~ at this station. The model data ~~coincides~~ validation
285 shows that, at other locations, the model represents temperatures generally well ~~with observational data~~, both at the surface
286 and in the lower layers. ~~Thus, in~~ In order to obtain further insights into ~~the~~ heat wave propagation towards the seafloor, we
287 analyzed the MYP model data (product ref. no. 3 in Table 1) along the entire water column.

288 A seasonal SST signal is clearly visible in Fig. ~~5a~~. In general, the temperature tends to decrease with depth while the bottom
289 temperature is relatively cold and uniform. In ~~late spring~~ early summer (June), a so-called cold intermediate layer (CIL) ~~at a~~
290 ~~depth of 20–60 m, which is~~, defined as a minimum of temperature between the thermocline and the perennial halocline
291 (Chubarenko et al., 2017; Dutheil et al., 2022), ~~is formed. The upper boundary of the CIL is in good agreement with the mixed~~
292 ~~layer depth. The CIL~~ 2022, develops at a depth of 20–60 m and acts as a barrier between the surface and bottom water ~~body~~
293 ~~and has~~ bodies. At Northern Baltic, the upper boundary of the CIL coincides with the mixed layer depth (MLD), which is
294 depicted in Fig. 5b-c. Starting from around June, a layer of water with a significantly lower temperature ~~(Fig. 5b) of 0.3 °C to~~
295 ~~4.5 °C as the climatological mean. As shown in Fig. 5c and Fig. 5d, the intensity of the MHW tends to decrease as the depth~~
296 ~~increases. MHWs in regions close to the seafloor were detected during specific periods from February to April, September to~~
297 ~~October and in December. During July, a one-day extreme MHW (Category IV) event was observed at the surface with 7.4 °C~~
298 ~~above the climatological mean temperature, followed by further three days with a severe MHW (Category III). A few weeks~~
299 ~~prior to this MHW (and in 10.8 m depth also afterwards), the temperature was already significantly higher than the~~
300 climatological mean, ~~but~~ (up to -7 °C deviation) is found just below the MLD (Fig. 5b), which suggests that the CIL was
301 significantly colder at this time in 2022. This also coincides with the onset of significantly higher temperatures at the surface
302 compared to the climatological mean, though these were initially not high enough to result in a MHW (Fig. ~~5e and 5f~~). The

303 elevated temperatures started with a significant temperature jump of 5-°C above the climatological mean, followed by an
304 abrupt and substantial ~~increases~~ and ~~decreases~~ in temperature over a short period (~~Fig. 5e~~). This eventually leads to a
305 MHW which lasts for 15 days starting from the end of June and which contains a one-day extreme MHW (Category IV) event
306 at a temperature of 7.4 °C above the climatological mean, followed by a severe MHW (Category III) for another three days.
307 Significantly high temperature deviations can also be observed at a depth of 10.8 m, i.e., at the MLD, after July 2nd, just after
308 the Category IV MHW at the surface. However, these temperature deviations did not result in a MHW at this depth. Following
309 this extreme heatwave event at the surface, a comparably weaker MHW is observed can be detected in mid-August. The
310 weaker August MHW is observable at both 0.5-m (Fig. 5e) and 10.8-m (Fig. 5f), while the June). Thus, this weaker MHW
311 is already no longer noticeable below the mixed layer depth. penetrates past the MLD into slightly deeper levels before reaching
312 the comparably cold layer of water underneath.
313 As shown in Fig. 5c and Fig. 5d, the intensity of the MHW tends to decrease as the depth increases. Four MHWs in regions
314 close to the seafloor (i.e., below 60 m) were detected during specific periods from February to April, September to October,
315 and in December. These MHWs are mostly moderate, with temperatures reaching up to 1.59 °C above the climatological mean.
316 Only three days at the end of September can be classified as a Category II MHW in one specific depth-layer close to the
317 seafloor. In the bottom-most depth-layer, the corresponding subsurface MHW is interrupted by five days of temperatures below
318 the 90th percentile. However, as the temperatures are only slightly below the threshold and the MHW criteria are still met in
319 the depth-layers above, one might still count this as one continuous MHW. Furthermore, Fig. 5c also shows isolated Category
320 I MHWs at depths between 20 and 50 m.

321 4 Discussion and Conclusions

322 During August and November 2022, record-warm sea surface temperatures were observed in substantial areas ~~in~~ of the Baltic
323 Sea proper. Large parts of the Baltic Sea exhibited the third-warmest to the warmest temperatures in summer ~~or~~ and autumn
324 temperatures months since 1997. Both periods, in August and November, coincided with atmospheric temperature anomalies.
325 In August air temperatures were higher than Over the 1991–2020 average across most of Europe, especially in Eastern Europe,
326 in a band stretching from the Barents and Kara seas to the Caucasus (Copernicus Climate Change Service/ECMWF, 2022a).
327 In November entire year of 2022, air temperatures were higher than the 1991–2020 average especially over the west, south-
328 east and far north of Europe and unusually mild over the northern European seas (Copernicus Climate Change
329 Service/ECMWF, 2022b). These atmospheric surface temperature anomalies are a likely driver for MHWs since they seem to
330 coincide with the observed marine surface temperature anomalies. Holbrook et al. (2019) found that the MHWs they studied
331 at middle and high latitude regions were driven by large scale atmospheric pressure anomalies which cause anomalous ocean
332 warming. Stalled ridges of atmospheric high pressure systems coincide with clear skies, warm air, and reduced wind speeds.
333 These conditions lead to quick warming of the upper ocean and increase thermal stratification due to reduced vertical mixing.

334 ~~In 2022, MHWs occurred in all marginal seas of Europe where the Baltic Sea was not an exception. The~~ distribution of
335 quantity and intensity of MHWs within the Baltic Sea is twofold: ~~Up~~ to seven individual MHW occurrences were ~~both~~
336 recorded ~~and as well as~~ simulated in the south-western part of the Baltic Sea, ~~which lead to the fact that and as a result~~ this
337 region experienced the maximum number of total MHW days ~~in the of anywhere in the Baltic Sea in 2022. In the northern~~
338 Baltic Sea ~~in 2022. In~~ the ~~northern part, the total~~ number of MHWs was lower, with ~~locally some locations registering~~ only
339 one MHW ~~being detected. Remarkably; remarkably, however,~~ this ~~one~~ MHW ~~also~~ led to the highest mean and maximum
340 MHW intensities in the Baltic Sea since the reanalysis started in 1993. In some areas, ~~in the Bothnian Bay, the Baltic Sea~~
341 ~~MYP revealed~~ temperatures ~~that~~ exceeded 9 °C above the 90th percentile of the climatologically expected temperature values.
342 ~~(Fig. 3d,e). This can be considered an extraordinarily high MHW intensity, since maximum SST anomalies above 5 °C have~~
343 ~~only been observed in about 5 % of the global ocean, and MHW intensities normally peak at 2.5 °C to 3.7 °C (Sen Gupta et~~
344 ~~al., 2020). In our case, the area in the Bothnian Bay experienced a short period with southerly winds and air temperatures up~~
345 ~~to 28 °C at the end of June 2022 (SMHI, 2023), which led to a short, but very intense MHW in the shallow areas of the Bay.~~
346 ~~At our two exemplary stations a~~ significant increase ~~of in~~ MHW occurrences is detectable over time: ~~at our two exemplary~~
347 ~~stations, of +0.773~~ MHW events per decade at LT Kiel and +0.64 MHW events per decade at Northern Baltic. ~~There is a~~
348 ~~statistical relationship between both~~ Both MHW frequency and ~~the~~ total number of MHW days ~~with are statistically related to~~
349 rising mean temperatures. This confirms that, ~~also in the Baltic Sea,~~ an increasing number of MHWs can be expected in the
350 future ~~in the Baltic Sea, too,~~ due to global warming (Frölicher et al., 2018; Oliver et al., 2019). ~~Adverse~~ ~~The adverse~~ impact of
351 MHWs ~~to different on the ecosystem's various~~ trophic levels ~~of the ecosystem is has been~~ widely documented (Smale et al.,
352 2019; IPCC, 2022; Smith et al., 2023). The Baltic Sea, which has a relatively vulnerable ecosystem, could experience ~~a~~
353 significant negative impact ~~due to from~~ MHWs (Kauppi and Villnäs, 2022; Kauppi et al., ~~2023~~–2023), and the analysis of
354 subsurface MHWs opens up further potential ways to study their effects. At the Northern Baltic mooring station, MHWs were
355 found ~~at the surface, propagating into deeper layers until reaching the CIL, and some were also detected close to the seafloor.~~
356 ~~Isolated MHWs were also observed at depths of between 20 and 50 m. However, these are subject to higher uncertainty~~
357 ~~compared to the ones in the surface and bottom layers due to a higher uncertainty in modeling variability in the pycnocline~~
358 ~~(QuID; Panteleit et al., 2023). Among the possible reasons for the development of the four MHWs close to the seafloor at~~
359 ~~Northern Baltic could be vertical heat transport from the surface or a lateral transport of warmer water due to bottom currents,~~
360 ~~for example. However, a more detailed evaluation would be required to assess their precise cause.~~
361 Potential ~~avenues~~ for future studies ~~opens up by include~~ examining whether ~~the August MHW in 2022 could and how surface~~
362 ~~MHWs are able to~~ propagate ~~into~~ the deeper water masses close to the halocline ~~at Northern Baltic and also regarding as well~~
363 ~~as examining~~ the correlation between the ~~strength (i.e., the classification category) of the MHW and its~~ propagation into deeper
364 water masses ~~and the strength (i.e. classification) of the MHW. Further.~~ At Northern Baltic, severe and extreme MHWs
365 occurred at the surface when the CIL was particularly cold compared to the climatology. This therefore raises questions of
366 ~~whether a strong CIL might be linked to the development of MHWs at the surface and whether the one might even favor the~~

367 ~~development of the other. Additional~~ studies could ~~determine if~~ also focus on the positive feedback on the bottom temperature,
368 ~~that~~ as was observed in 2022~~,. It might be interesting to determine if this phenomenon~~ can also be found in ~~following other~~
369 years and whether ~~this phenomenon it~~ is triggered by the superposition of ~~either~~ lateral currents ~~and/or~~ MHWs~~, or of both~~
370 ~~together~~. Understanding the effects that potentially lead to the vertical propagation of MHWs~~, like those observed~~ particularly
371 in ~~the~~ late summer~~, of 2022~~ will become increasingly crucial in order to evaluate ~~the effects of~~ how the already ~~rising~~
372 ~~occurrence-increasing occurrences~~ of surface MHWs ~~may affect the ecosystem in subsurface layers~~.

373 Appendix A1

374 We apply a clustering approach to evaluate the precision of the hydrodynamic model. This technique offers insights into the
375 overall accuracy of the model by grouping the errors. The clustering procedure employs the K-means algorithm, a type of
376 unsupervised machine learning (Jain, 2010). The original explanation of this technique can be found in a study by Raudsepp
377 and Maljutenko (2022). In our evaluation, all available data within the model's domain and simulation period are considered,
378 even if the observation data is unevenly distributed or occasionally sparse. This strategy enables us to assess the model's quality
379 at each specific location and time instance at which measurements have been acquired.

380 Initially, a two-dimensional error space (dS , dT) was established using simultaneously-measured temperature and salinity
381 values as the foundation for clustering. Here, $dS=(S_{mod}-S_{obs})$ and $dT=(T_{mod}-T_{obs})$ represent the differences between the model
382 (S_{mod} and T_{mod}) and observed (S_{obs} and T_{obs}) salinity and temperature, respectively. The dataset employed in this validation
383 study was sourced from the EMODNET dataset compiled by SMHI (product ref. [no. 4](#) in Table 1). It consists of a total of
384 3,094,089 observations aligning with the simulation period of the Baltic Sea physics reanalysis (product ref. [no. 3](#) in Table 1)
385 and covering the years 1993 to 2022. For each observation, we extracted the nearest model values from the reanalysis dataset.
386 The next stage involves choosing the number of clusters, and for simplicity we opted in advance for five clusters. Subsequently,
387 the third step entails conducting K-means clustering on the two-dimensional errors. This clustering process is applied to the
388 normalized errors achieved through separate normalization for temperature and salinity errors using the corresponding standard
389 deviations. The K-means algorithm then identifies the centroids' positions within the error space for the predetermined number
390 of clusters. These centroids' locations signify the bias of the error set for each cluster. In the fourth step, statistical metrics for
391 non-normalized clustered errors are computed. Standard deviation (STD), root mean square deviation (RMSD) and the
392 correlation coefficient are examples of common statistics that can be calculated for the parameters associated with each cluster.
393 The fifth step involves examining the spatio-temporal distributions of errors associated with different clusters. During the
394 creation of the error space, we retained the coordinates of each error point (dS , dT)(x , y), allowing us to map the errors of each
395 cluster back onto the locations where the measurements were conducted. To achieve this, the model domain is partitioned into
396 horizontal grid cells (i , j) of 27×27 km² in size. Subsequently, the number of error points attributed to various clusters at each
397 grid cell (i , j) is tallied. The total number of error points linked to the grid cell (i , j) is the sum of points from each cluster. The

398 proportion of error points in each grid cell affiliated with cluster k is determined by the ratio of the number of error points of
399 cluster k to the total number of error points in each grid cell.

400
401 Figure ~~respect~~A1 displays the results of the K-means clustering for non-normalized errors. Table S1 presents the corresponding
402 metrics. Within cluster k=5, the salinity and temperature values closely align with the observations, with a bias of $dS=-$
403 0.40 g/kg and $dT=-0.02$ °C, respectively. This cluster encompasses 57 % of all data points. The points are distributed
404 throughout the Baltic Sea and the great majority of them exceed 0.5 (Figure A1b). Clusters k=3 and k=4 exhibit relatively even
405 spatial distributions across the Baltic Sea, accounting for 11 % and 8 % of the points, respectively. These clusters are
406 particularly noteworthy due to their relatively high temperature biases and variability, both of which are crucial for the
407 calculation of marine heatwaves. The clusters k=1 and k=2 represent points with low temperature but a high salinity error
408 (Table A1). Spatially, these points are predominantly located in the southwestern Baltic Sea (Figure A1b), which points to the
409 occasional underestimation or overestimation of the inflow/outflow salinity.
410 Collectively, approximately 82 % of all validation points exhibit relatively low temperature bias, STD and RMSD (Table A1).
411 The surface-layer validation shows that less than 10 % of comparison points have significant temperature errors (Figure A1c).
412 Due to the low proportion of these validation points, we do not expect a significant impact on the ~~ecosystem in subsurface~~
413 layers ~~determination~~ of surface MHWs and their statistics. Below the surface layer, i.e., at depths ranging from 0.5–40 m, up
414 to 25 % of the points correspond to clusters k=3 and k=4 (Figure A1c). Consequently, we anticipate that the model reanalysis
415 data provides sufficiently accurate information for calculating subsurface MHWs and their statistics for the Baltic Sea.

416 **Data availability**

417 This study is based on public databases and the references are listed in Table 1.

418 **Author contribution**

419 The idea for and concept of ~~behind~~ this chapter ~~was~~ were formed by Anja Lindenthal, Claudia Hinrichs, Priidik Lagemaa, Helen
420 E. Morrison and Urmas Raudsepp. The data curation was done by Eefke M. van der Lee and Tim Kruschke for the data from
421 product ref. no. 1 in Table 1, by Claudia Hinrichs and Tabea R. Panteleit for the data from product ref. no. 2 in Table 1 and by
422 Simon Jandt-Scheelke and Tabea R. Panteleit for the data from product ref. no. 3 in Table 1. The formal analyses of the datasets
423 and the resulting investigations were performed by Anja Lindenthal, Claudia Hinrichs, Simon Jandt-Scheelke, Tim Kruschke
424 and Tabea R. Panteleit. Additional The k-means model validation was performed by Tabea R. Panteleit-Urmas Raudsepp and
425 Ilja Maljutenko. Claudia Hinrichs, Simon Jandt-Scheelke, Ilja Maljutenko, Tim Kruschke and Tabea R. Panteleit were
426 responsible for the visualization of the data. Anja Lindenthal, Claudia Hinrichs, Simon Jandt-Scheelke, Tim Kruschke, Eefke

427 M. van der Lee, Tabea R. Panteleit and Urmas Raudsepp were involved in the original draft preparation, ~~while the~~ The final
428 manuscript was ~~finally~~ reviewed and edited by Claudia Hinrichs, Priidik Lagemaa, Helen E. Morrison and Urmas Raudsepp
429 with contributions from all co-authors.

430 **Competing interests**

431 The authors declare that they have no conflict of interest.

432 **Funding**

433 This work is supported by the Copernicus Marine Service for the Baltic Sea Monitoring and Forecasting Center (21002L2-
434 COP-MFC BAL-5200).

435 **References**

436 Belkin, I. M.: Rapid warming of large marine ecosystems. *Progress in Oceanography*, 81(1-4), 207-213,
437 <https://doi.org/10.1016/j.pocean.2009.04.011>, 2009.

438 [Buga, L., Sarbu, G., Fryberg, L., Magnus, W., Wesslander, K., Gatti, J., Leroy, D., Iona, S., Larsen, M., Koefoed Rømer, J.,](#)
439 [Østrem, A. K., Lipizer, M., and Giorgetti A.: EMODnet Chemistry Eutrophication and Acidity aggregated datasets v2018,](#)
440 [EMODnet, Thematic Lot no. 4/SI2.749773, https://doi.org/10.6092/EC8207EF-ED81-4EE5-BF48-E26FF16BF02E, 2018.](#)

441 Cheng, L., von Schuckmann, K., Abraham, J. P., et al.: Past and future ocean warming, *Nature Reviews Earth and*
442 *Environment*, 3(11), 776-794, <https://doi.org/10.1038/s43017-022-00345-1>, 2022.

443 Chubarenko, I. P., Demchenko, N. Y., Esiukova, E. E., Lobchuk, O. I., Karmanov, K. V., Pilipchuk, V. A., Isachenko, I. A.,
444 Kuleshov, A. F., Chugaevich, V. Y., Stepanova, N. B. et al.: Spring thermocline formation in the coastal zone of the
445 southeastern Baltic Sea based on field data in 2010–2013. *Oceanology*, 57, 632–638,
446 <https://doi.org/10.1134/S000143701705006X>, 2017.

447 Copernicus Climate Change Service/ECMWF, <https://climate.copernicus.eu/surface-air-temperature-august-2022>, last access:
448 11 July 2023, 2022a.

449 Copernicus Climate Change Service/ECMWF, <https://climate.copernicus.eu/surface-air-temperature-november-2022>, last
450 access: 11 July 2023, 2022b.

- 451 Dutheil, C., Meier, H. E. M., Gröger, M., Börgel, F.: Warming of Baltic Sea water masses since 1850, *Climate Dynamics*,
452 <https://doi.org/10.1007/s00382-022-06628-z>, 2022.
- 453 EU Copernicus Marine Service Product: Global Ocean- In-Situ Near-Real-Time Observations, Mercator Ocean International,
454 [data set], <https://doi.org/10.48670/moi-00036>, 2022a.
- 455 EU Copernicus Marine Service Product: Baltic Sea - L3S Sea Surface Temperature Reprocessed, Mercator Ocean
456 International, [data set], <https://doi.org/10.48670/moi-00312>, 2022b.
- 457 EU Copernicus Marine Service Product: Baltic Sea Physics Reanalysis, Mercator Ocean International, [data set],
458 <https://doi.org/10.48670/moi-00013>, 2023.
- 459 EUMETSAT, AVHRR Factsheet, Doc.No.: EUM/OPS/DOC/09/5183, <https://www.eumetsat.int/media/39253>, 2015.
- 460 Frölicher, T. L., Fischer, E. M., Gruber, N.: Marine heatwaves under global warming, *Nature*, 560, 360–364,
461 <https://doi.org/10.1038/s41586-018-0383-9>, 2018.
- 462 [Giorgetti, A., Lipizer, M., Molina Jack, M. E., Holdsworth, N., Jensen, H. M., Buga, L., Sarbu, G., Iona, A., Gatti, J., Larsen,](#)
463 [M., and Fyrberg, L.: Aggregated and Validated Datasets for the European Seas: The Contribution of EMODnet Chemistry,](#)
464 [Front. Mar. Sci., 7, 583657, https://doi.org/10.3389/fmars.2020.583657, 2020.](#)
- 465 Goebeler, N., Norkko, A., Norkko, J.: Ninety years of coastal monitoring reveals baseline and extreme ocean temperatures are
466 increasing off the Finnish coast, *Commun. Earth Environ.*, 3, 215, <https://doi.org/10.1038/s43247-022-00545-z>, 2022.
- 467 Gröger, M., Placke, M., Meier, H. E. M., Börgel, F., Brunnabend, S.-E., Dutheil, C., Gräwe, U., Hieronymus, M., Neumann,
468 T., Radtke, H., Schimanke, S., Su, J., Väli, G.: The Baltic Sea Model Intercomparison Project (BMIP) – a platform for model
469 development, evaluation, and uncertainty assessment, *Geosci. Model Dev.*, 15, 8613–8638, [https://doi.org/10.5194/gmd-15-](https://doi.org/10.5194/gmd-15-8613-2022)
470 [8613-2022](#), 2022.
- 471 Gurvan, M., Bourdallé-Badie, R., Chanut, J., Clementi, E., Coward, A., Ethé, C., Iovino, D., Lea, D., Lévy, C., Lovato, T.,
472 Martin, N., Masson, S., Mocavero, S., Rousset, C., Storkey, D., Vancoppenolle, M., Müeller, S., Nurser, G., Bell, M., Samson,
473 G.: NEMO ocean engine. In Notes du Pôle de modélisation de l'Institut Pierre-Simon Laplace (IPSL) (v4.0, Number 27).
474 Zenodo. <https://doi.org/10.5281/zenodo.3878122>, 2019.
- 475 Hobday, A. J., Alexander, L. V., Perkins, S. E., Smale, D. A., Straub, S. C., et al.: A hierarchical approach to defining marine
476 heatwaves, *Prog. Oceanogr.*, 141, 227–38, <https://doi.org/10.1016/j.pocean.2015.12.014>, 2016.

477 Hobday, A. J., Oliver, E. C. J., Sen Gupta, A., Benthuisen, J. A., Burrows, M. T., Donat, M. G., Holbrook, N. J., Moore, P. J.,
478 Thomsen, M. S., Wernberg, T., Smale, D. A.: Categorizing and naming marine heatwaves, *Oceanography*, 31(2), 162–173,
479 <https://doi.org/10.5670/oceanog.2018.205>, 2018.

480 Holbrook, N.J., Scannell, H.A., Sen Gupta, A., Benthuisen, J.A., Feng, M., Oliver, E.C., Alexander, L.V., Burrows, M.T.,
481 Donat, M.G., Hobday, A.J. and Moore, P.J.. A global assessment of marine heatwaves and their drivers. *Nature*
482 *communications*, 10(1), p.2624. <https://doi.org/10.1038/s41467-019-10206-z>. 2019.

483 ICES Bottle and low-resolution CTD dataset, Extractions 22 DEC 2013 (for years 1990-20012), 25 FEB 2015 (for year 2013),
484 13 OCT 2016 (for year 2015), 15 JAN 2019 (for years 2016-2017), 22 SEP 2020 (for year 2018), 10 MAR 2021 (for years
485 2019-202), 28 FEB 2022 (for year 2021), ICES, Copenhagen, 2022.

486 In Situ TAC partners: EU Copernicus Marine Service Product User Manual for the Global Ocean- In-Situ Near-Real-Time
487 Observations Product, INSITU_GLO_PHYBGCWAV_DISCRETE_MYNRT_013_030, Issue 1.14, Mercator Ocean
488 International, <https://catalogue.marine.copernicus.eu/documents/PUM/CMEMS-INS-PUM-013-030-036.pdf>, last access: 12
489 April 2023, 2022.

490 IPCC: Climate Change 2022: Impacts, Adaptation, and Vulnerability. Contribution of Working Group II to the Sixth
491 Assessment Report of the Intergovernmental Panel on Climate Change, eds.: Pörtner, H.-O., Roberts, D. C., Tignor, M.,
492 Poloczanska, E. S., Mintenbeck, K., Alegría, A., Craig, M., Langsdorf, S., Löschke, S., Möller, V., Okem, A., Rama, B.,
493 Cambridge University Press, Cambridge, UK and New York, NY, USA, 3056 pp., <https://doi.org/10.1017/9781009325844>,
494 2022.

495 Jain, A. K.: Data clustering: 50 years beyond K-means, *Pattern Recognition Letters*, 31(8), 651-666,
496 <https://doi.org/10.1016/j.patrec.2009.09.011>, 2010.

497 Kauppi, L., Villnäs, A.: Marine heatwaves of differing intensities lead to distinct patterns in seafloor functioning, *Proceedings*
498 *of the Royal Society B: Biological Sciences*, 289(1986), 20221159, <https://doi.org/10.1098/rspb.2022.1159>, 2022.

499 Kauppi, L., Göbeler, N., Norkko, J., Norkko, A., Romero-Ramirez, A., Bernard, G.: Changes in macrofauna bioturbation
500 during repeated heatwaves mediate changes in biogeochemical cycling of nutrients, *Frontiers in Marine Science*, 9, 1070377,
501 <https://doi.org/10.3389/fmars.2022.1070377>, 2023.

502 Minnett, P. J., Alvera-Azcárate, A., Chin, T. M., Corlett, G. K., Gentemann, C. L., Karagali, I., Li, X., Marsouin, A., Marullo,
503 S., Maturi, E., Santoleri, R., Saux Picart, S., Steele, M., Vazquez-Cuervo, J.: Half a century of satellite remote sensing of sea-

504 surface temperature, Remote Sensing of Environment, 233, 111366, ISSN 0034-4257,
505 <https://doi.org/10.1016/j.rse.2019.111366>, 2019.

506 Oliver, E. C. J.: marineHeatWaves v0.16, github [code], <https://github.com/ecjoliver/marineHeatWaves>, 2016.

507 Oliver, E. C. J.: Mean warming not variability drives marine heatwave trends, Clim. Dyn., 53, 1653–1659,
508 <https://doi.org/10.1007/s00382-019-04707-2>, 2019.

509 Panteleit, T., Verjovkina, S., Jandt-Scheelke, S., Spruch, L. and Huess, V.: EU Copernicus Marine Service Quality Information
510 Document for the Baltic Sea Physics Reanalysis Product, BALTICSEA_MULTIYEAR_PHY_003_011, Issue 4.0, Mercator
511 Ocean International, <https://catalogue.marine.copernicus.eu/documents/QUID/CMEMS-BAL-QUID-003-011.pdf>, last
512 access: 12 April 2023, 2023.

513 Raudsepp, U., Maljutenko, I., Haapala, J., Männik, A., Verjovkina, S., Uiboupin, R., von Schuckmann, K., Mayer, M.: Record
514 high heat content and low ice extent in the Baltic Sea during winter 2019/20. In: Copernicus Ocean State Report, Issue 6,
515 Journal of Operational Oceanography, 15:sup1, s175–s185, <https://doi.org/10.1080/1755876X.2022.2095169>, 2022.

516 [Raudsepp, U., Maljutenko, I.: A method for assessment of the general circulation model quality using K-means clustering](#)
517 [algorithm: a case study with GETM v2.5, Geosci Model Dev., 15, 535–551, https://doi.org/10.5194/gmd-15-535-2022, 2022.](#)

518 Ringgaard, I., Korabel, V., Spruch, L., Lindenthal, A. and Huess, V.: EU Copernicus Marine Service Product User Manual for
519 the Baltic Sea Physics Reanalysis Product, BALTICSEA_MULTIYEAR_PHY_003_011, Issue 1.0, Mercator Ocean
520 International, https://catalogue.marine.copernicus.eu/documents/PUM/CMEMS-BAL-PUM-003-011_012.pdf, last access:
521 12 April 2023, 2023.

522 [Sen Gupta, A., Thomsen, M., Benthuyesen, J.A. et al.: Drivers and impacts of the most extreme marine heatwave events, Sci](#)
523 [Rep 10, 19359, https://doi.org/10.1038/s41598-020-75445-3, 2020.](#)

524 She, J., Su, J., Zinck, A.-S.: Anomalous surface warming in the Baltic Sea in summer 2018 and mechanism analysis, In:
525 Copernicus Marine Service Ocean State Report, Issue 4, Journal of Operational Oceanography, 13:sup1, s125–s132;
526 <https://doi.org/10.1080/1755876X.2020.1785097>, 2020.

527 Smale, D. A., Wernberg, T., Oliver, E. C. J., et al.: Marine heatwaves threaten global biodiversity and the provision of
528 ecosystem services, Nature Climate Change, 9(4), 306-312, <https://doi.org/10.1038/s41558-019-0412-1>, 2019.

529 [SMHI: Baltic Sea – Eutrophication and Acidity aggregated datasets 1902/2017 v2018. Aggregated datasets were generated in](#)
530 [the framework of EMODnet Chemistry III, under the support of DG MARE Call for Tender EASME/EMFF/2016/006 – lot4,](#)
531 [EMODnet Chemistry \[data set\], <https://doi.org/10.6092/595D233C-3F8C-4497-8BD2-52725CEFF96B>, 2019.](#)

532 [SMHI: Meteorological observations \[data set\], air temperature, station number 140480 \(Umeå Flygplats\),](#)
533 [https://www.smhi.se/data/meteorologi/ladda-ner-meteorologiska-](https://www.smhi.se/data/meteorologi/ladda-ner-meteorologiska-observationer/#param=airtemperatureInstant,stations=core,stationid=140480)
534 [observationer/#param=airtemperatureInstant,stations=core,stationid=140480](https://www.smhi.se/data/meteorologi/ladda-ner-meteorologiska-observationer/#param=airtemperatureInstant,stations=core,stationid=140480), last access: 19 Dec 2023, 2023.

535 Smith, K. E., Burrows, M. T., Hobday, A. J., King, N. G., Moore, P. J., Gupta, A. S., Thomsen, M. S., Wernberg, T., Smale,
536 D. A.: Biological Impacts of Marine Heatwaves. *Annual Review of Marine Science*, 15 (1), 119–145.
537 <https://doi.org/10.1146/annurev-marine-032122-121437>, 2023.

538 Sun, D., Jing, Z., Li, F., Wu, L.: Characterizing global marine heatwaves under a spatio-temporal framework, *Progress in*
539 *Oceanography*, 211, 102947, <https://doi.org/10.1016/j.pocean.2022.10294>, 2023.

540 The BACC Author Team: Assessment of Climate Change for the Baltic Sea Basin, Springer Berlin, Heidelberg, p. 88,
541 <https://doi.org/10.1007/978-3-540-72786-6>, 2008.

542 Väli, G., Meier, H. M., Elken, J.: Simulated halocline variability in the Baltic Sea and its impact on hypoxia during 1961–
543 2007, *J. Geophys. Res. Oceans*, 118, 6982-7000, <https://doi.org/10.1002/2013JC009192>, 2013.

544 Wehde, H., Schuckmann, K. V., Pouliquen, S., Grouazel, A., Bartolome, T., Tintore, J., De Alfonso Alonso-Munoyerro, M.,
545 Carval, T., Racapé, V. and the INSTAC team: EU Copernicus Marine Service Quality Information Document for the Global
546 Ocean- In-Situ Near-Real-Time Observations Product, INSITU_GLO_PHYBGCWAV_DISCRETE_MYNRT_013_030,
547 Issue 2.2, Mercator Ocean International, [https://catalogue.marine.copernicus.eu/documents/QUID/CMEMS-INS-QUID-013-](https://catalogue.marine.copernicus.eu/documents/QUID/CMEMS-INS-QUID-013-030-036.pdf)
548 [030-036.pdf](https://catalogue.marine.copernicus.eu/documents/QUID/CMEMS-INS-QUID-013-030-036.pdf), last access: 12 April 2023, 2022.

549 WMO: State of the Global Climate 2022, WMO-No. 1316, World Meteorological Organization, 2023, 48 pp., 2023.

550 Zhao, Z., Marin, M.: A MATLAB toolbox to detect and analyze marine heatwaves, *Journal of Open Source Software*, 4(33),
551 1124, <https://doi.org/10.21105/joss.01124>, 2019.

552

Tables

553

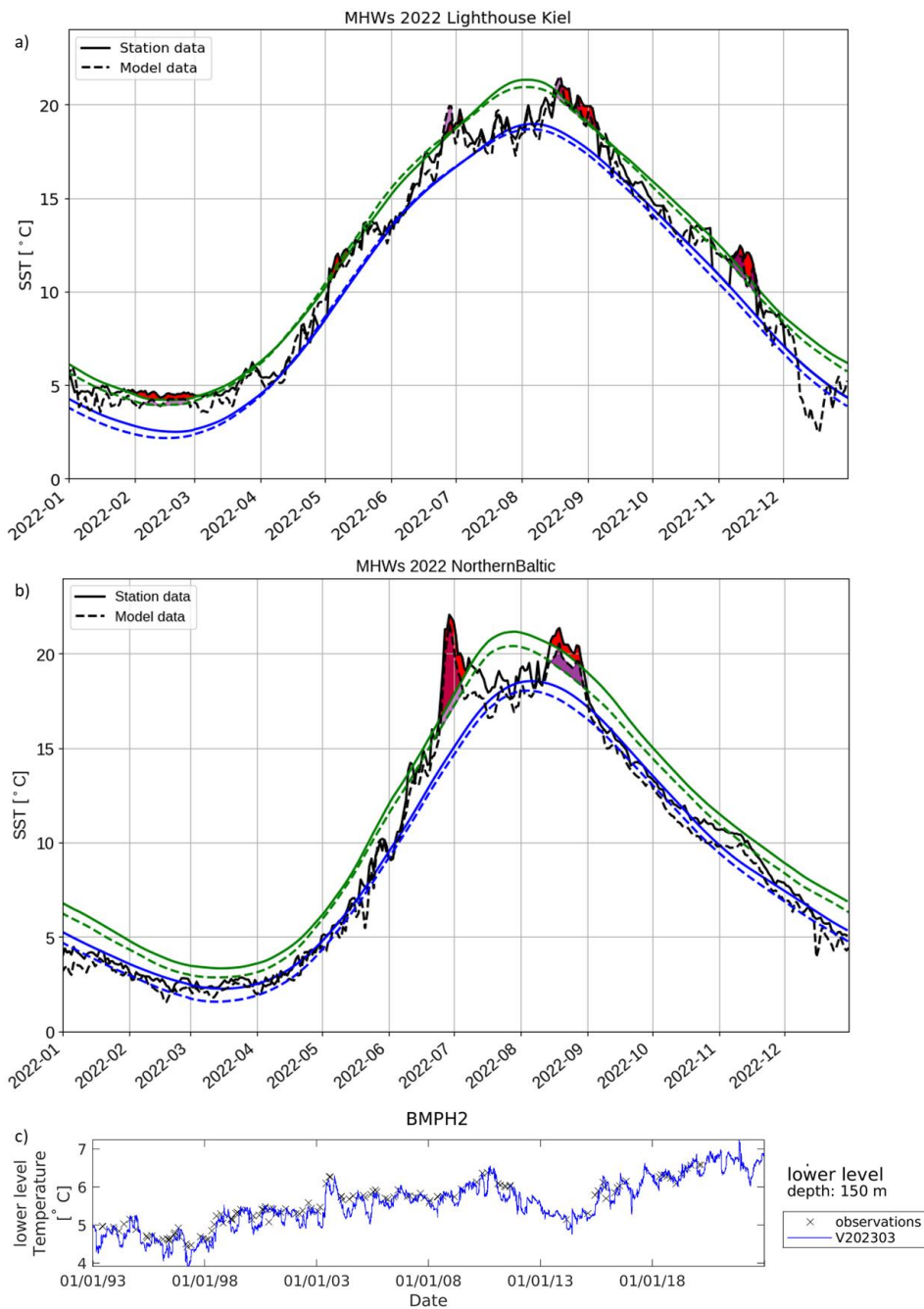
554

Table 1: Product Table

Product ref. no.	Product ID & type	Data access	Documentation
1	BSH Sea Surface Temperature (AVHRR/3); Satellite data	Upon request; overview and contact data via https://www.bsh.de/EN/TOPICS/Monitoring_systems/Remote_sensing/remote_sensing_node.html	https://www.bsh.de/DE/THEMEN/Beobachtungssysteme/Fernerkundung/fernerkundung_node.html
2	INSITU_GLO_PHYBGCWAV_DISCRETE_MYNRT_013_030; In-Situ Near-Real-Time Observations	EU Copernicus Marine Service Product (2022a)	Quality Information Document (QUID): Wehde et al., 2022 Wehde et al. (2022) Product User Manual (PUM): In Situ TAC partners, 2022 In Situ TAC partners (2022)
3	BALTICSEA_MULTIYEAR_PHY_003_011; Numerical models	EU Copernicus Marine Service Product (2023)	Quality Information Document (QUID): Panteleit et al., 2023 Panteleit et al. (2023) Product User Manual (PUM): Ringgaard et al., 2023 Ringgaard et al. (2023)
4	EMODNET CHEMISTRY Baltic Sea aggregated eutrophication and acidity datasets 1902-2017 v2018; Observations	SMHI (2019)	Buga et al. (2018) , Giorgetti et al. (2020)

555

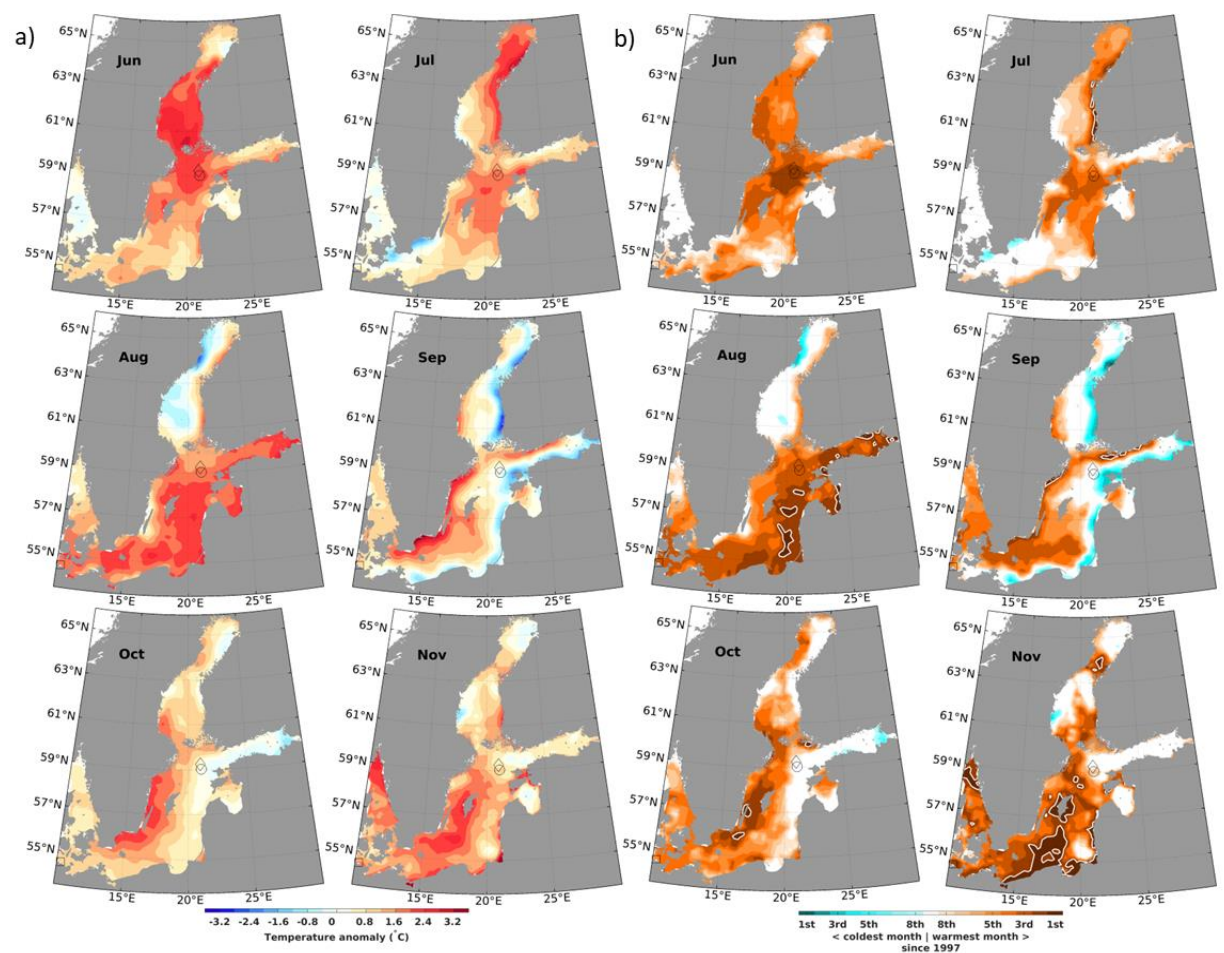
556



557
 558 **Figure 1: Comparison of station data with model data at (a) LT Kiel (product ref. no. 2 and 3 in Table 1), (b) Northern Baltic**
 559 **(product ref. no. 2 and 3 in Table 1) and (c) BMPH2 (from Panteleit et al., 2023). The dashed lines in (a) and (b) correspond to the**
 560 **model (product ref. no. 3 in Table 1), while the continuous lines correspond to the station data (product ref. no. 2 in Table 1). In**
 561 **blue, the climatological mean is shown. The green lines show the 90th percentile threshold for MHW detection and the black lines**
 562 **are the respective 2022 temperature data. The purple (model data) and red (station data) marked areas show the detected MHWs**

563
564
565

~~in 2022~~. The reference period for LT Kiel (a) is 1993–2021 and 1997–2021 for Northern Baltic (b). (c) shows the validation at the station BMPH2 at a depth of 150 m. The model data is shown in blue and the measured data are displayed with the black crosses.



566
567
568

Table 2: Pearson correlation coefficients from linear regression between the MHW metrics computed from the station data and the model data at the stations Lighthouse Kiel and Northern Baltic.

<u>Station</u>	<u>common climatology period</u>	<u>MHW count</u>	<u>MHW max intensity</u>	<u>MHW cumulative intensity</u>	<u>total MHW days</u>
<u>Lighthouse Kiel</u>	<u>1993-2021</u>	<u>0.82</u>	<u>0.88</u>	<u>0.66</u>	<u>0.93</u>
<u>Northern Baltic</u>	<u>1997-2021</u>	<u>0.74</u>	<u>0.89</u>	<u>0.82</u>	<u>0.94</u>

569
570

Table 3: Statistical MHW parameter values in various subregions of the Baltic Sea for 2022 based on the model data from the Baltic Sea MYP (product ref. no. 3 in Table 1) using daily values of SST between 1st January 1993 and 31st December 2022. The climatological period covers the years 1993 to 2021.

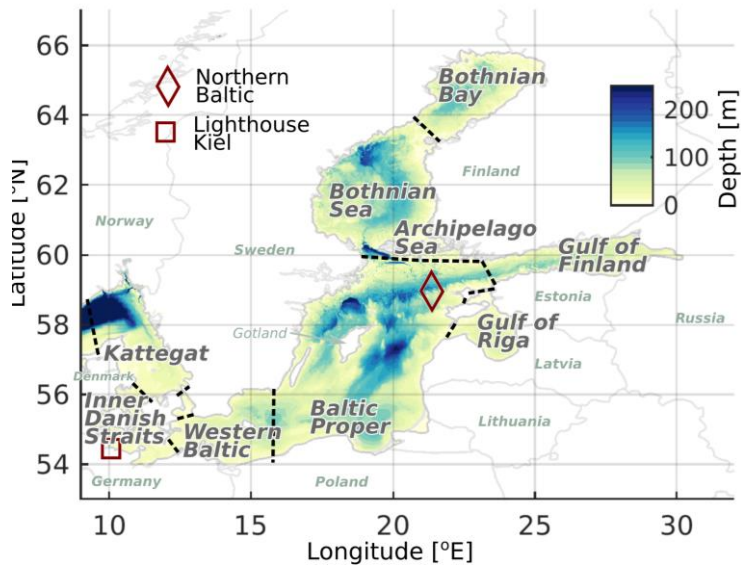
	<u>Kattegat</u>	<u>Inner Danish Straits</u>	<u>Western Baltic</u>	<u>Baltic Proper</u>	<u>Gulf of Riga</u>	<u>Gulf of Finland</u>	<u>Archiipelago Sea</u>	<u>Bothnian Sea</u>	<u>Bothnian Bay</u>
<u>Cumulative intensity of longest MHW / °C days</u>	<u>81.5</u>	<u>63.8</u>	<u>64</u>	<u>79.4</u>	<u>63</u>	<u>66.5</u>	<u>61.1</u>	<u>119.3</u>	<u>85.1</u>
<u>Mean intensity / °C</u>	<u>3.6</u>	<u>3.5</u>	<u>3.8</u>	<u>5.3</u>	<u>4.9</u>	<u>5.8</u>	<u>4.5</u>	<u>6.4</u>	<u>6.5</u>
<u>Duration of longest MHW / days</u>	<u>24</u>	<u>29</u>	<u>26</u>	<u>32</u>	<u>17</u>	<u>17</u>	<u>21</u>	<u>31</u>	<u>20</u>
<u>Number of MHWs (modal) per year</u>	<u>1-6 (3)</u>	<u>2-7 (4)</u>	<u>2-7 (5)</u>	<u>1-7 (3)</u>	<u>1-4 (3)</u>	<u>1-4 (2)</u>	<u>2-4 (3)</u>	<u>1-6 (2)</u>	<u>1-5 (2)</u>
<u>Maximum intensity / °C</u>	<u>4.5</u>	<u>4.2</u>	<u>4.6</u>	<u>7.3</u>	<u>5.9</u>	<u>6.8</u>	<u>5.1</u>	<u>8.6</u>	<u>9.6</u>
<u>Total days of MHW conditions / days</u>	<u>56</u>	<u>86</u>	<u>94</u>	<u>79</u>	<u>50</u>	<u>48</u>	<u>55</u>	<u>63</u>	<u>47</u>

Table A1: The share (%), bias, root-mean-square error (RMSE), standard deviation (SD), and correlation coefficient (Corr) for each of the five clusters.

<u>k</u>	<u>Shares</u> <u>%</u>	<u>Bias</u>		<u>SD</u>		<u>RMSE</u>		<u>Corr</u>		
		<u>dS</u> <u>(g/kg)</u>	<u>dT</u> <u>(°C)</u>	<u>dS</u> <u>(g/kg)</u>	<u>dT</u> <u>(°C)</u>	<u>S</u> <u>(g/kg)</u>	<u>T</u> <u>(°C)</u>	<u>S</u>	<u>T</u>	<u>dSdT</u>
<u>1</u>	<u>18.6</u>	<u>-4.14</u>	<u>-0.26</u>	<u>1.80</u>	<u>0.85</u>	<u>4.51</u>	<u>0.89</u>	<u>0.90</u>	<u>0.78</u>	<u>-0.09</u>
<u>2</u>	<u>7.4</u>	<u>3.53</u>	<u>0.39</u>	<u>2.16</u>	<u>1.06</u>	<u>4.14</u>	<u>1.13</u>	<u>0.93</u>	<u>0.75</u>	<u>-0.11</u>
<u>3</u>	<u>10.5</u>	<u>-0.62</u>	<u>2.58</u>	<u>2.12</u>	<u>1.28</u>	<u>2.21</u>	<u>2.88</u>	<u>0.97</u>	<u>0.58</u>	<u>-0.06</u>
<u>4</u>	<u>6.3</u>	<u>0.27</u>	<u>-2.29</u>	<u>1.97</u>	<u>1.21</u>	<u>1.99</u>	<u>2.59</u>	<u>0.95</u>	<u>0.71</u>	<u>-0.14</u>
<u>5</u>	<u>57.2</u>	<u>-0.40</u>	<u>-0.02</u>	<u>0.83</u>	<u>0.54</u>	<u>0.92</u>	<u>0.54</u>	<u>0.99</u>	<u>0.89</u>	<u>0.07</u>

578

Figures



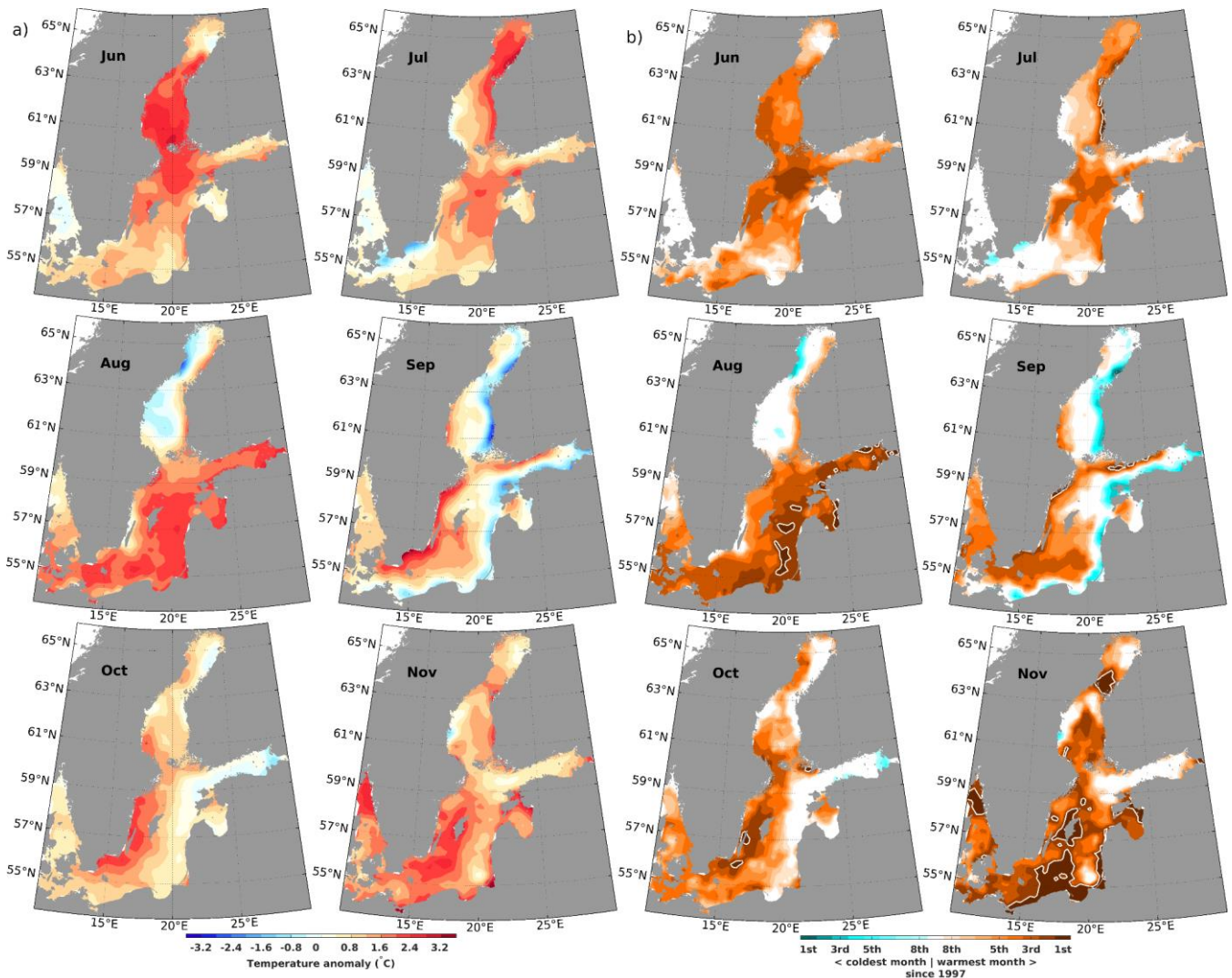
579

Figure 1: Map of the Baltic Sea with relevant locations mentioned in the study. Boundaries between subregions are marked with dashed lines.

580

581

582



583

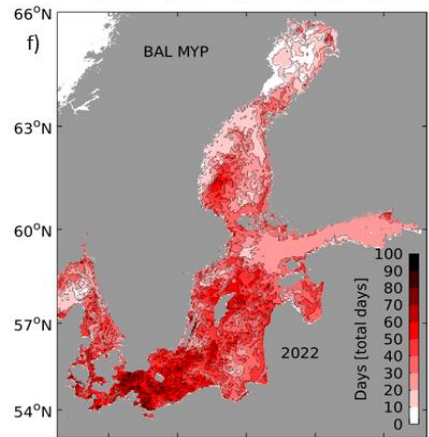
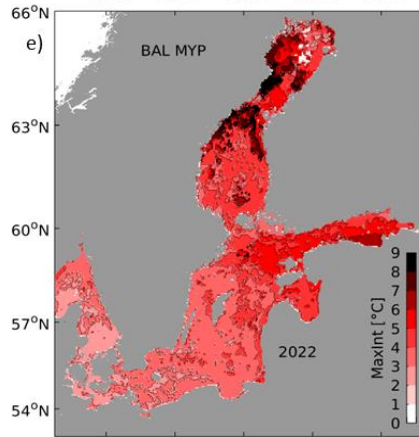
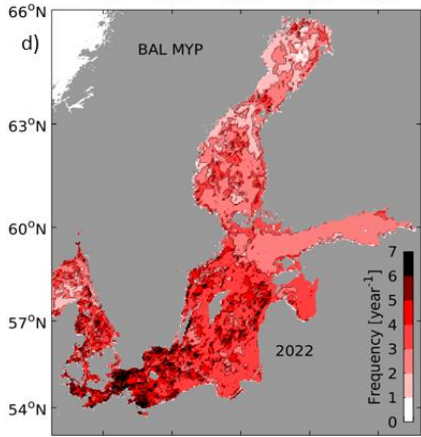
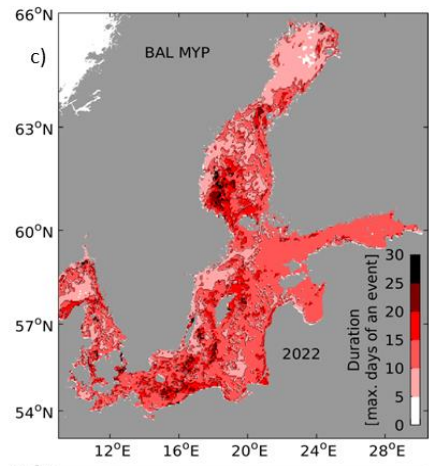
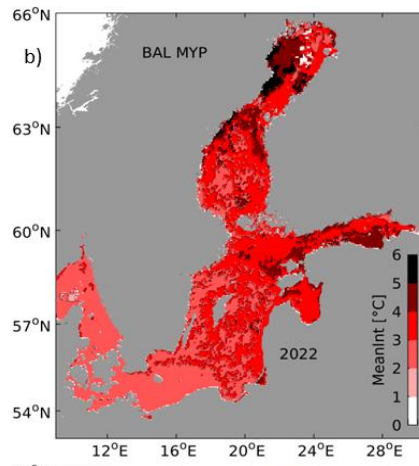
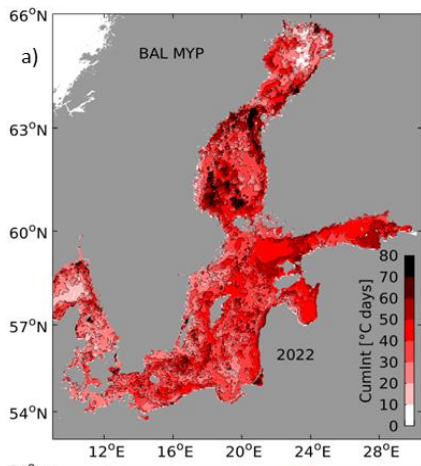
584

Figure 2:

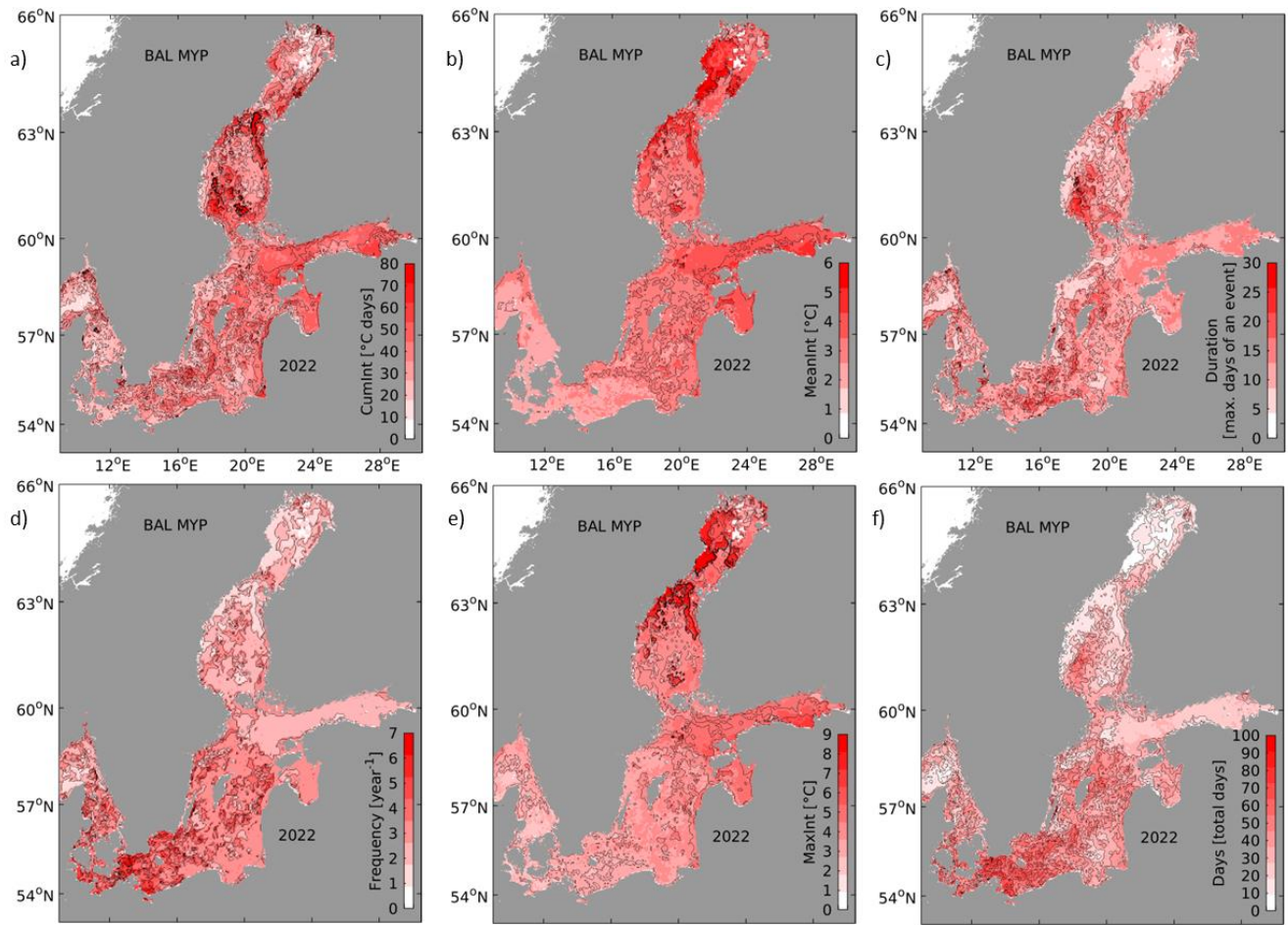
585

Figure 2: Anomalies (difference to climatology of 1997-2021) of SST for the Baltic Sea according to the BSH SST analysis (product ref. no 1 in Table 1) during the summer and autumn months in 2022 (a) and ranks of these SST anomalies (b) when compared to the full dataset starting in 1997. In (b), **B**rownish (cyan) colors denote anomalies belonging to the warmest (coldest) eight anomalies found since 1997. Record warm anomalies (rank 1) are highlighted by white contours. ~~Locations of the in situ observations discussed in this chapter are marked by a square (LT Kiel), a diamond (Northern Baltic), and a circle (BMPH2), respectively.~~

589



590

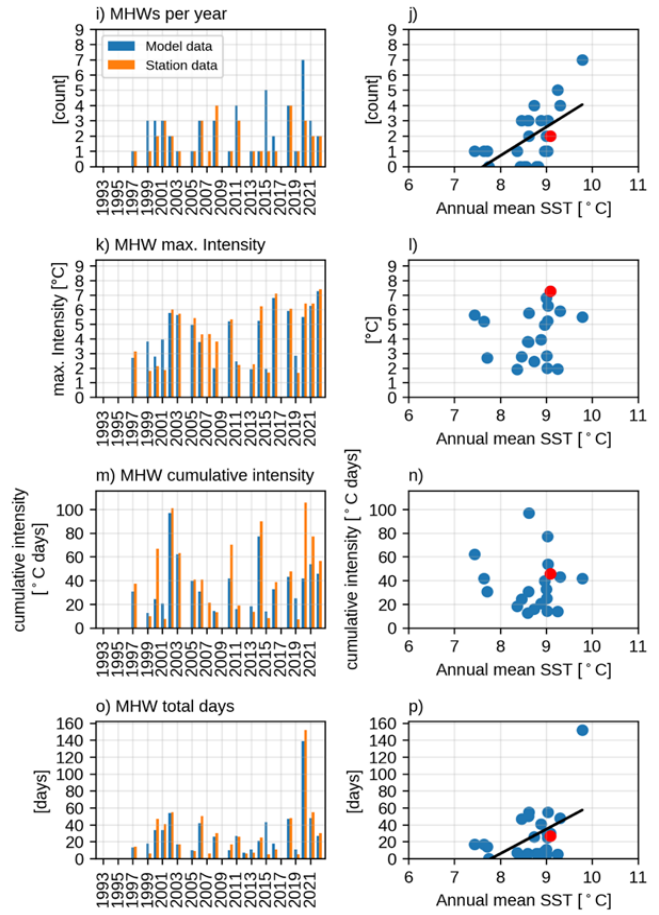
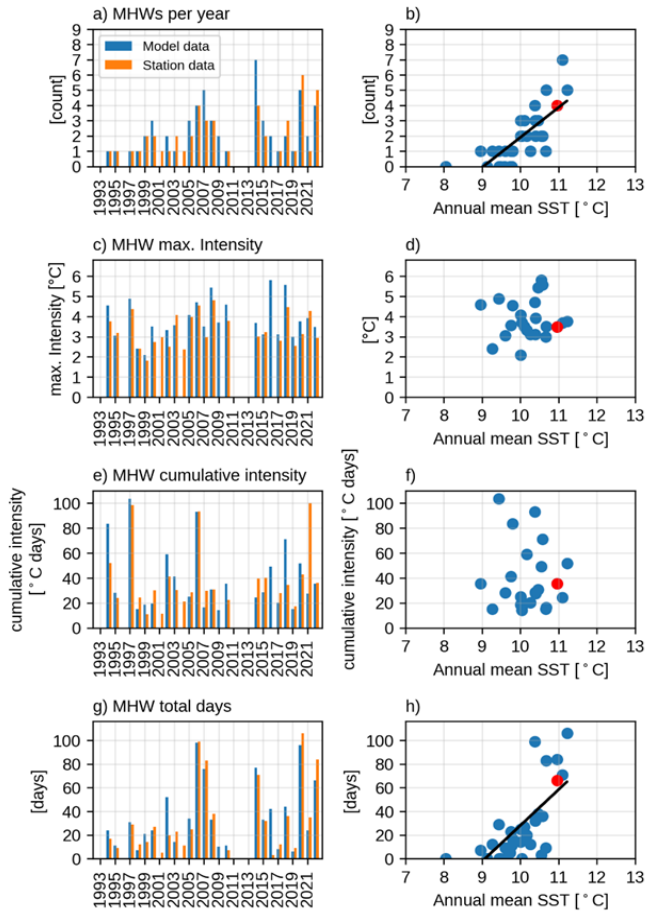


591

592 **Figure 13:** Statistical metrics of MHWs in 2022 in the Baltic Sea based on SST data of the Baltic Sea MYP (product ref. no. 3 in
 593 Table 1) with the climatological period covering the years 1993 to 2021 - (a) cumulative intensity of the longest heatwave, (b) mean
 594 intensity, (c) duration of the longest heatwave, (d) number of heatwaves during 2022, (e) maximum intensity during the longest
 595 heatwave, (f) summed up days of all heatwave during 2022. The definition of these metrics follows Hobday et al. (2016).

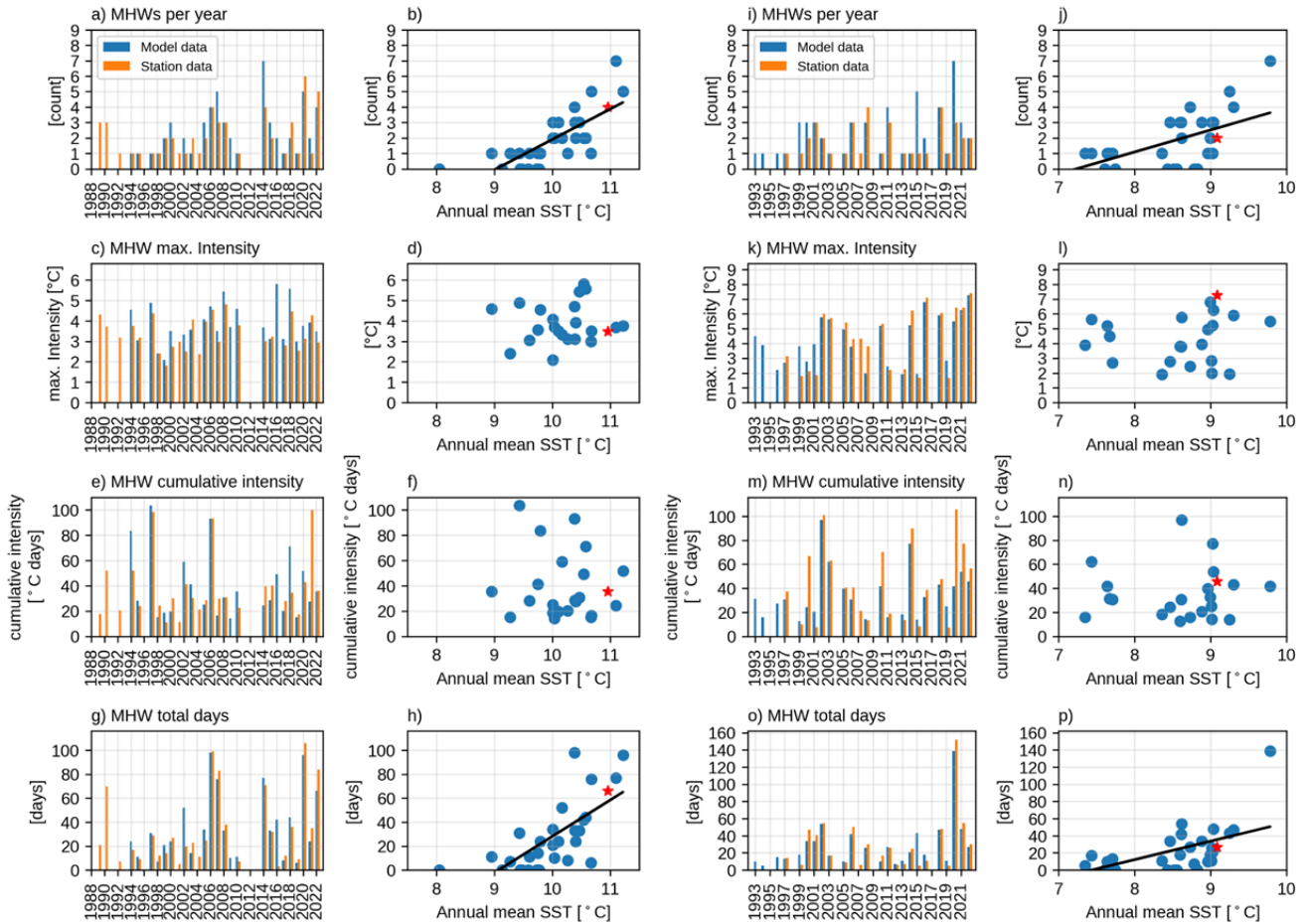
LT Kiel

Northern Baltic



LT Kiel

Northern Baltic



597

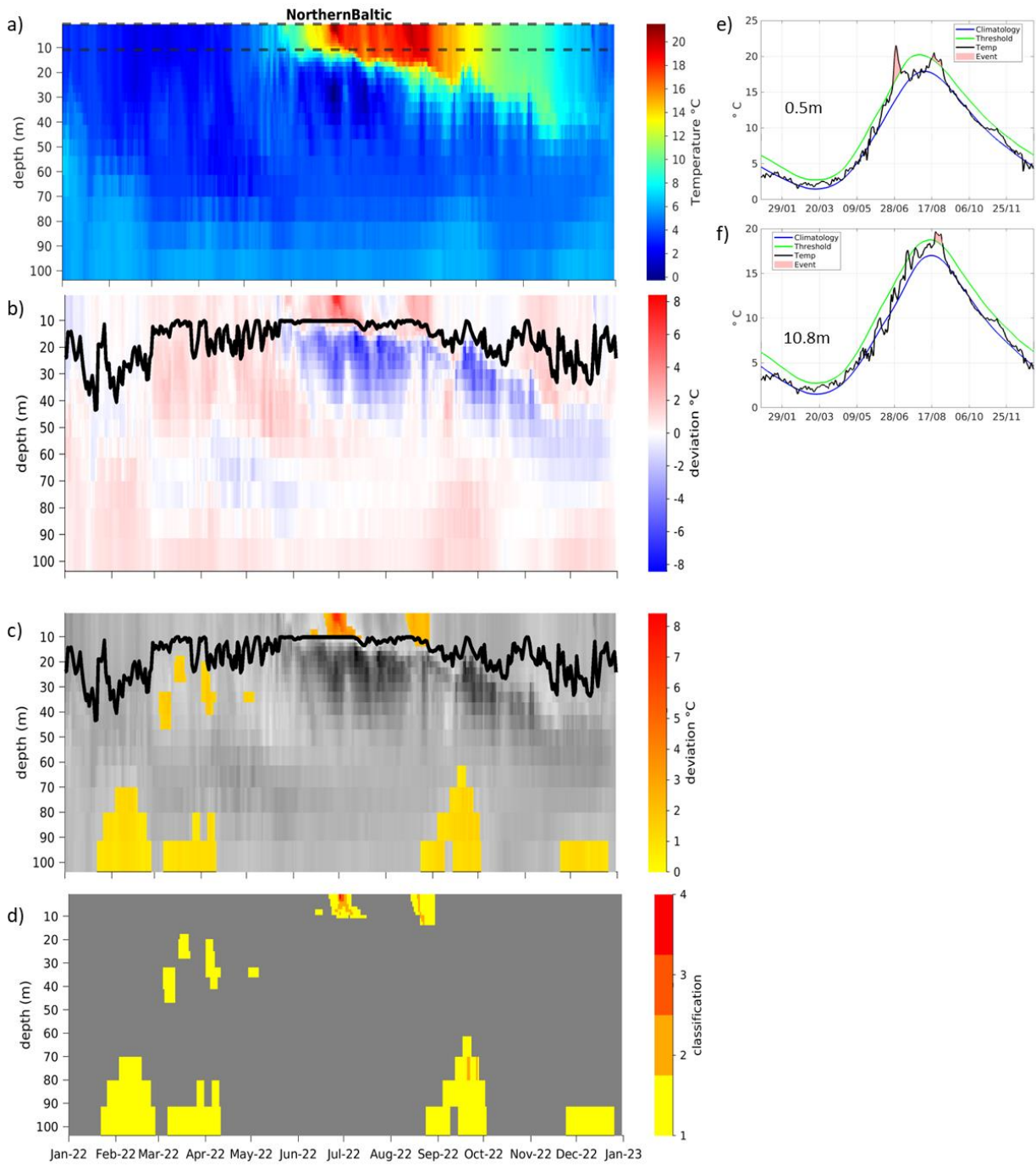
598

599

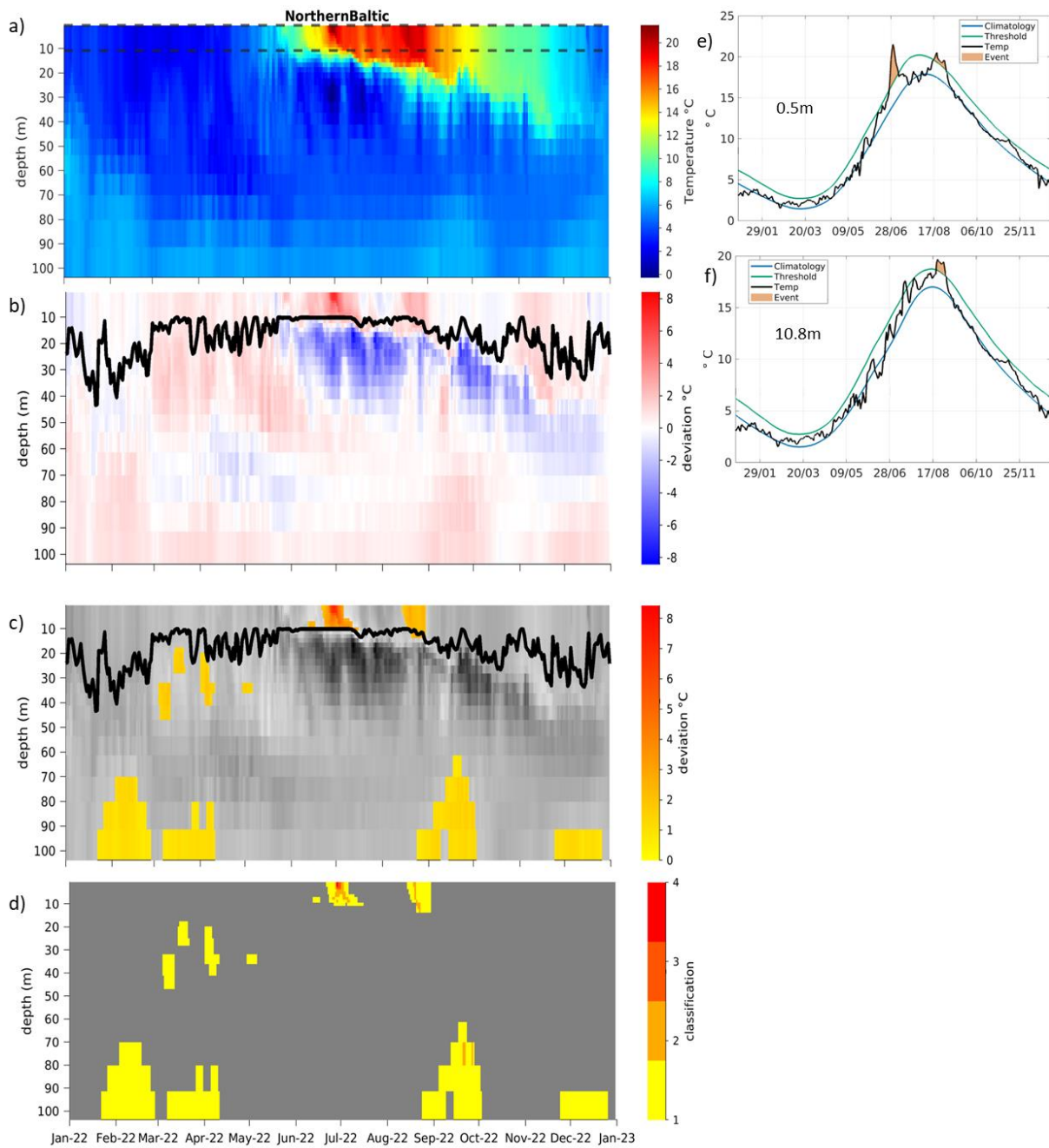
600

601

Figure 24: Comparison and time series of annual MHW metrics (a,i: MHW events; c,k: maximum intensity [°C]; e,m: cumulative intensity [°C days]; g,o: MHW days) for station data (orange bars) and model data (blue bars) at the stations LT Kiel (left) and Northern Baltic (right). The MHW metrics from the model are plotted against the annual mean SST at that station with the year 2022 marked in red. Statistically significant (95 %) correlations are indicated with a black line.



602

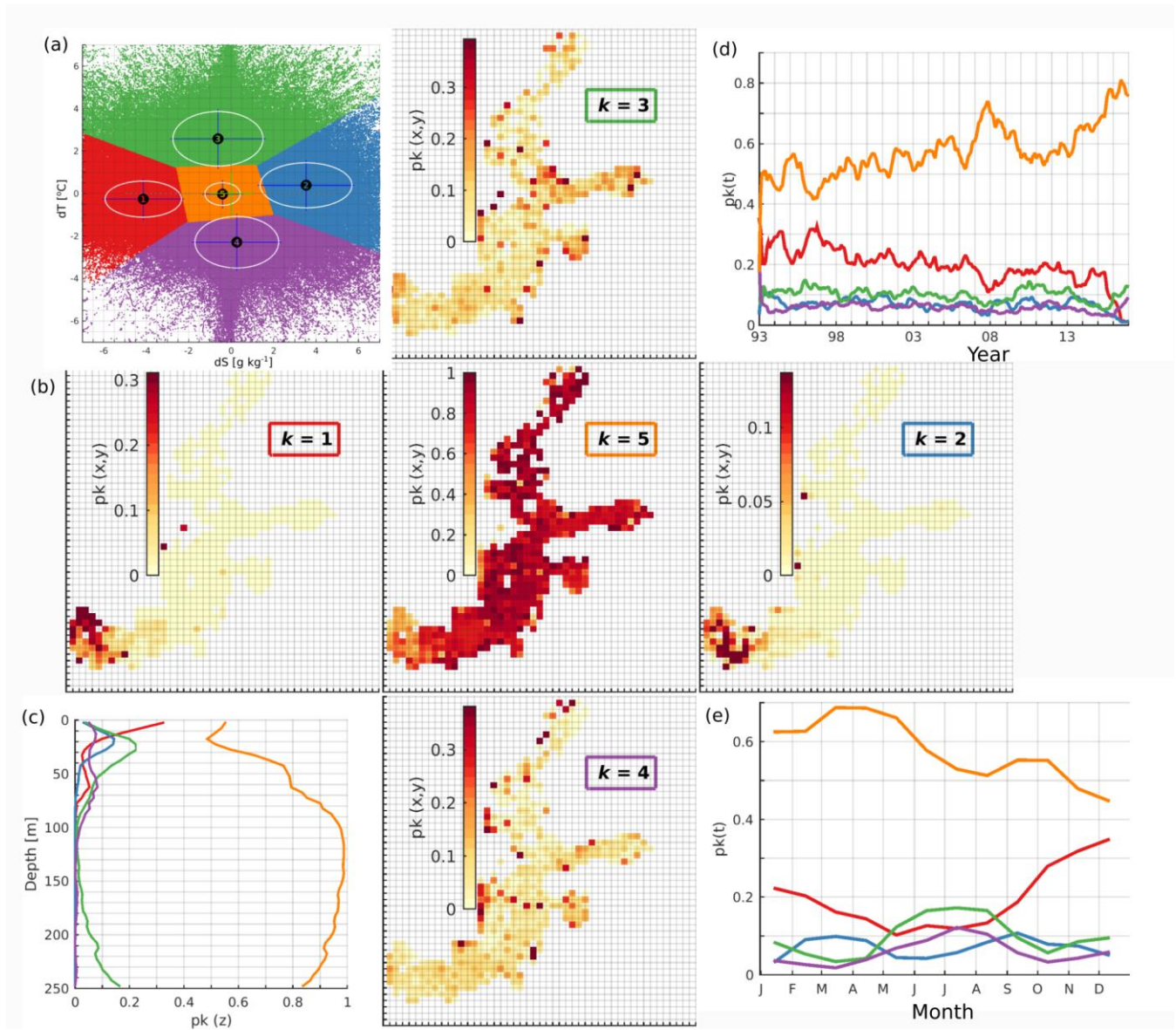


603

604 **Figure 35:** Hovmöller diagrams show absolute water temperature (a), temperature anomalies deviation between the climatology
 605 and the MYP data for 2022 (b) and MHWs (c) and their classifications (d, 1-moderate, 2-strong, 3-severe, 4-extreme) including the
 606 mixed layer depth as the thick black line (b and c) at Northern Baltic based on the Baltic Sea MYP (product ref. no. 3 in Table 1).
 607 The time series on the right (e-f) are located at the vertical positions marked as dashed lines in (a) and show SST temperature

608
609

(black), climatology (blue), 90th percentile threshold for MHW analysis (green) and MHWs (red shading) based on model data at depths of 0.5 m (e), 10.8 m (f), 80.1 m (g) and 103.8 m (h). The period used for the climatology is 1993-2021.

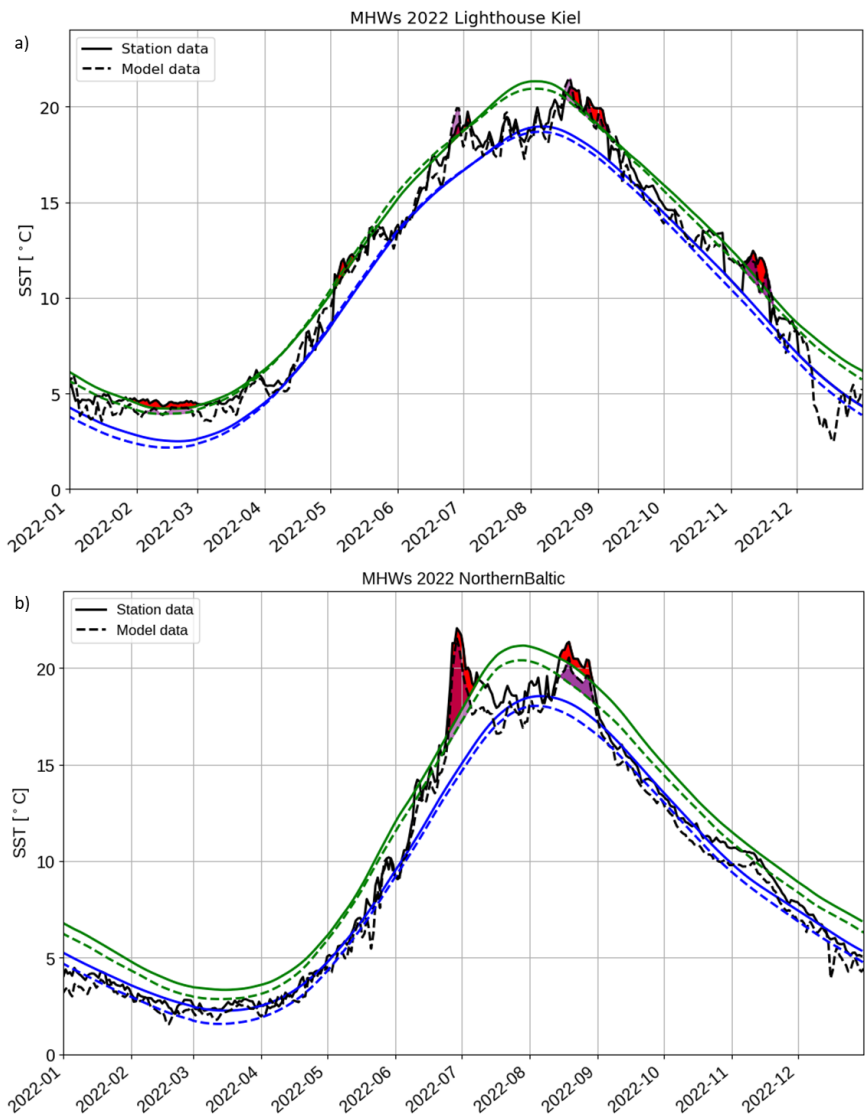


610

611

612

Figure A1: Distribution of normalized error clusters for $k=5$ (a). The spatial distribution (b, shaded sub-plots), vertical distribution (c), temporal distribution (d), and seasonal distribution (e) of the share of error points belonging to the five different clusters.



613

614 **Figure A2: Comparison of station data with model data at (a) LT Kiel (product ref. no. 2 and 3 in Table 1), (b) Northern Baltic (K. Hedi, FMI, pers. communication and product ref. no. 3 in Table 1). The dashed lines correspond to the model, while the continuous**
 615 **lines correspond to the station data. In blue, the climatological mean is shown. The green lines show the 90th percentile threshold**
 616 **for MHW detection and the black lines are the respective 2022 temperature data. The purple (model data) and red (station data)**
 617 **marked areas show the detected MHWs in 2022. The reference period is 1993-2021 for LT Kiel (a) and 1997-2021 for Northern**
 618 **Baltic (b).**
 619